reliable validity with regard to the relationship between clinical symptoms and the prediction of total hip surgery. At entry into this study, the Kellgren-Lawrence score was determined by one observer (N.S.), an orthopedic surgeon with more than 20 years of experience in the treatment of hip osteoarthritis.

The average ages of the volunteers and patients were 28 years (range, 23–40 years) and 39 years (range, 24–50 years), respectively. The average weight and body mass index were 53 kg (range, 47–59 kg) and 20.8 kg (range, 18.9–23.2), respectively, for the volunteers and 56 kg (range, 43–70 kg) and 21.9 kg (range, 18.9–29.5), respectively, for the patients. There were no significant differences between the volunteers and patients with respect to weight and body mass index; however, the volunteers were significantly younger than the patients with hip dysplasia ($P = .004$).

At study entry, the center-edge angle of patients was measured on anteroposterior radiographs by one observer (N.S.). The center-edge angle, as measured on radiographs, ranged from −10° to 16° (mean, 4.7°). Six hips were classified as being in the prearthritic stage (grade 0), and nine were classified as being in the early arthritic stage (grade 1 or 2). Three patients had no pain in their hips, and 12 patients had slight or moderate pain in their hips either while walking or after a long walk. The volunteers did not undergo radiography. The center-edge angle of both patients and volunteers was measured on midcoronal MR images by one observer (N.S.). The interval between measurements performed on MR images and measurements performed on radiographs was at least 1 month. All volunteers had center-edge angles of more than 25° (range, 26°–34°) on midcoronal MR images. In patients, the center-edge angles on midcoronal MR images ranged from −8° to 17° (mean, 5°).

Clinical symptoms of the hip were evaluated in all participants by using the pain score of the Western Ontario and McMaster Universities (WOMAC) osteoarthritis questionnaire (31). The WOMAC pain score was calculated as the summation of the scores ranging from 0 (no pain) to 4 (extreme pain) in response to each of the five items (total score range, 0–20). The WOMAC score was determined by one musculoskeletal clinician (N.S).

### MR Imaging

Patients and volunteers were instructed to limit strenuous weight-bearing activity (eg, running or ascending stairs for a long distance) 3 hours before MR imaging. All subjects were instructed to sit on a chair for at least 20 minutes before MR imaging. A unilateral hip joint was imaged under loaded and unloaded conditions by using a 3.0-T MR unit with a flexible surface coil (Signa; GE Healthcare, Milwaukee, Wis). The right hip was examined in eight patients and the left hip was examined in seven. The volunteers were randomly assigned for imaging at the right hip in five volunteers and at the left hip in four.

During MR imaging, the volunteers and patients were supine with the hip in a neutral position on a custom-made loading apparatus consisting of a back board and a sliding foot plate on low-friction rollers (Fig 1). Under the loaded condition, axial compression force was transmitted to the hip joint cranially by means of the foot plate, which was connected to a water-filled weight.

The correlation between the water volume in the tanks and the actual force applied to the foot with the foot plate was confirmed in a preliminary examination: When seven different amounts of water volume, set up evenly over a range of 15–45 kg, were examined, there was a high correlation between the water volume and the actual force applied to the foot plate, which was measured by using a spring balance ($r = 0.998$, $P < .0001$). Under the loaded condition, an axial compression force was transmitted to the hip joint by applying 50% of the body weight only to the examined leg, assuming that this would simulate loading conditions in the static standing position.

Coronal T2 maps were obtained under the loaded and unloaded conditions from two-dimensional dual-spin-echo images with the following parameters: repetition time msec/echo time msec, 1500/10 and 45; field of view, 16 cm; matrix, 512 × 256 interpolated to 512 × 512 with a resulting in-plane pixel resolution of 312.5 μm; section thickness, 5 mm; and two signals acquired for a total imaging time of 13.5 minutes. Coronal T2 maps from two-dimensional multiple-spin-echo images (repetition time, 1500 msec; eight evenly spaced echoes between 11 and 88 msec; field of

**Figure 1**

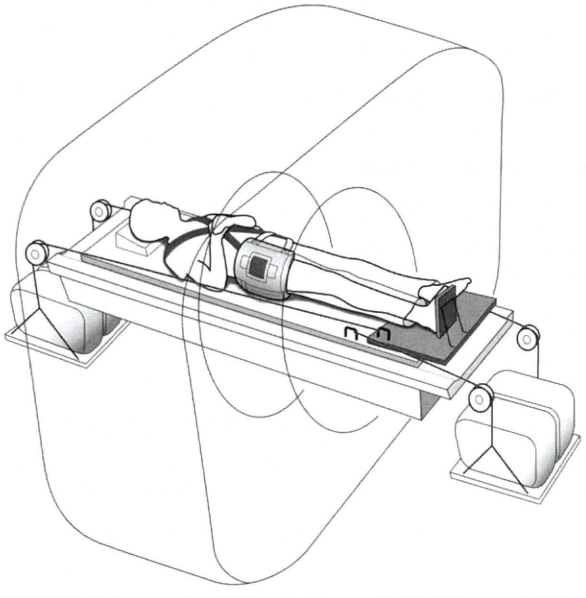

**Figure 1:** Schematic of the custom-made loading apparatus used during MR imaging. The foot of the examined leg was secured in a neutral rotational position by strapping it tightly to a sliding foot rest plate. The subject's shoulders were strapped tightly to the back board. Under the loading condition, axial compression force was transmitted to the hip joint cranially by means of the foot plate, which was connected to a water-filled weight. The same magnitude of counterforce was also applied to the back board caudally to prevent cranial displacement of the body.

view, 16 cm; matrix, 384 × 256; section thickness, 5 mm; two signals acquired; total imaging time, 13 minutes) were also obtained under the unloaded condition. Owing to inferior in-plane resolution, however, the coronal T2 maps from multiple-spin-echo images were used only to examine the correlation of measured T2 values with those from dual-spin-echo images. A frequency-selective fat-suppression technique was used to minimize the chemical shift artifact at the cartilage-bone interface. Frequency encoding was oriented in the cranial-to-caudal direction. First, MR images were obtained with the dual-spin-echo sequence and the multiple-spin-echo sequence under the unloaded condition by using the same axial localizing images. Then, the load was applied for an average of 6 minutes (range, 5–7 minutes), after which MR images were obtained with the dual-spin-echo sequence under the continuously loaded condition. The imaging planes were co-registered by comparing the positions on axial localizing images and coronal trial images under the loaded and unloaded conditions.

### MR Imaging Data Analysis

All analyses were performed with use of the coronal images through the center of the femoral head by using custom-developed software (Baum, version 1.00; Osaka University, Osaka, Japan). The T2 value was calculated on a pixel-by-pixel basis by fitting the echo time data and corresponding signal intensity to a monoexponential equation. In the calculation of T2 values from the multiple-spin-echo images, the first echo was excluded to minimize T2 inaccuracy due to stimulated echoes (32,33). The acetabular and femoral cartilages at weight bearing were manually defined on the image corresponding to the first echo from the lateral border of the acetabular fossa to the lateral margin of the acetabulum (Fig 2). Attention was paid not to include joint fluid with high signal intensity at the surface of the acetabular and femoral cartilages on the image with the second or later echo time. Each acetabular and femoral cartilage was automatically divided into three radial sections with equal widths

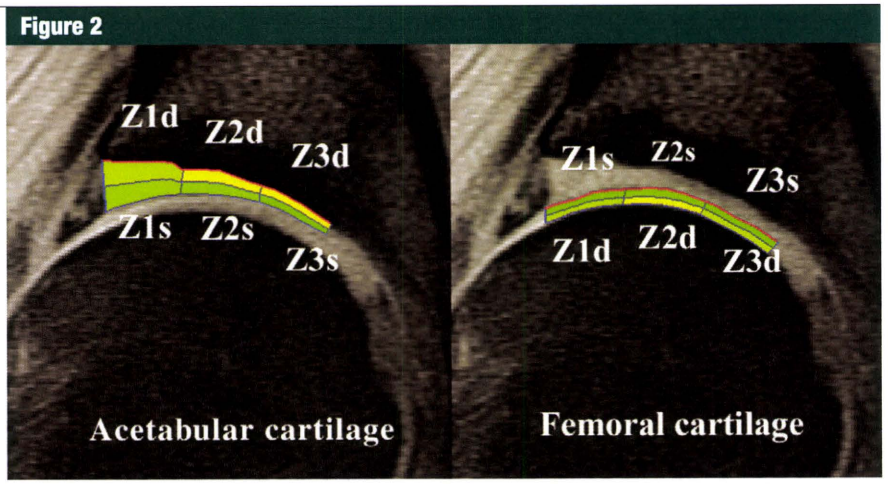


**Figure 2:** Images illustrate the ROIs at the weight-bearing area in the acetabular cartilage and femoral cartilage. Femoral cartilage zones Z3d and Z3s were excluded from analysis because of the frequent involvement of the ligamentum teres at the insertion to the femoral head in patients with hip dysplasia.

(zones Z1, Z2, and Z3), and each section was further divided into deep layers (zones Z1d, Z2d, and Z3d) and superficial layers (zones Z1s, Z2s, and Z3s) with equal thickness. Zones Z3d and Z3s of the femoral cartilage were excluded from analysis because of the frequent involvement of the ligamentum teres at the insertion into the femoral head in dysplastic hips. The average T2 value of each subdivided region of interest (ROI) (zones Z1s, Z1d, Z2s, Z2d, Z3s, and Z3d) and the average cartilage thickness of each ROI (zones Z1, Z2, Z3) were calculated. ROIs were measured three times, and the average T2 value and cartilage thickness were determined by one observer (T.N., with more than 10 years of experience in the study of articular cartilage imaging), who was blinded to the radiologic assessments.

*Reliability of T2 measurements from dual-spin-echo images.*—To assess reliability in the calculation of T2 values from dual-spin-echo images that were used in the subsequent analysis, the relationships between T2 values from dual-spin-echo images and T2 values from multiple-spin-echo images at each zone under the unloaded condition were evaluated by using the Spearman correlation coefficient.

*Reproducibility of T2 and cartilage thickness measurements.*—To assess the reproducibility of measurements, an additional observer (T.S., with 3 years of experience in articular cartilage imaging), who was blinded to the radiologic assessments, independently evaluated cartilage T2 and cartilage thickness from dual-spin-echo MR images under unloaded conditions in 10 subjects—the first five volunteers and the first five patients. The interobserver reproducibility in cartilage T2 and thickness at each ROI was calculated from the measurements by the two observers (T.N. and T.S.) as the coefficient of variation (expressed as percentage: [standard deviation/mean] × 100), and the mean reproducibility was calculated as the root-mean-square average of the 10 cases.

### Statistical Analysis

Statistical analysis was performed by one observer (H.T., with 10 years of experience in the study of radiology) by using standard software (SPSS, version 11; SPSS, Chicago, Ill). Descriptive analysis was performed to evaluate the WOMAC pain scores, the reliability of T2 measurements with dual-spin-echo images versus that with multiple-spin-echo images, and the reproducibility of measurements between the two observers. Cartilage T2 values and cartilage thickness at each ROI under the unloaded and loaded conditions were compared between the volunteers and patients by using the nonparametric Mann-Whitney *U* test. In both volunteers and patients, cartilage T2 values and cartilage

**Table 1**

**Relationships between Dual-Spin-Echo and Multiple-Spin-Echo T2 at Each Acetabular and Femoral Cartilage Zone**

| Zone | T2 with Two Echoes (msec)* | T2 with Multiple Echoes (msec)* | *r* Value | *P* Value |
|---|---|---|---|---|
| Acetabular cartilage | | | | |
| Z1d | 23.9 ± 3.4 | 35.4 ± 4.8 | 0.72 | .0005 |
| Z1s | 33.7 ± 4.6 | 43.7 ± 6.1 | 0.83 | .0001 |
| Z2d | 23.5 ± 3.7 | 34.7 ± 5.0 | 0.74 | .0004 |
| Z2s | 34.2 ± 4.0 | 45.1 ± 6.0 | 0.78 | .0002 |
| Z3d | 26.5 ± 6.2 | 42.1 ± 7.9 | 0.78 | .0002 |
| Z3s | 37.9 ± 6.1 | 51.4 ± 9.0 | 0.85 | .0001 |
| Femoral cartilage | | | | |
| Z1d | 26.2 ± 3.3 | 32.7 ± 4.4 | 0.62 | .0028 |
| Z1s | 36.1 ± 4.0 | 44.1 ± 4.4 | 0.67 | .0014 |
| Z2d | 26.1 ± 5.3 | 33.0 ± 3.9 | 0.60 | .0038 |
| Z2s | 35.5 ± 5.3 | 43.8 ± 7.2 | 0.82 | .0001 |

* Data are given as means ± standard deviations.

thickness under the unloaded condition were compared with those under the loaded condition by using the Wilcoxon signed rank test. Changes in T2 values and cartilage thickness at each ROI with loading were compared between the volunteers and patients by using the nonparametric Mann-Whitney *U* test. Among the patients, the relationships between the changes in T2 with loading and age, body mass index, and center-edge angle on radiographs were evaluated by using the Spearman correlation coefficient. A *P* value of less than .05 was indicative of statistical significance.

## Results

At MR imaging, a WOMAC pain score of 0 was determined in all hips of the healthy volunteers; the average WOMAC pain score of the dysplastic hips was 3.5 (range, 0–9).

Compared with T2 values from multiple-spin-echo images, T2 values from dual-spin-echo images at the corresponding zone showed lower mean values under the unloaded condition (Table 1). Results of Spearman correlation coefficient analysis showed significant correlations between both T2 values at all zones, with *r* values of 0.60–0.85.

The interobserver reproducibility of T2 measurements in the acetabular cartilage was as follows: Z1d, 2.2%; Z1s, 2.3%; Z2d, 2.6%; Z2s, 1.2%; Z3d, 5.8%; and Z3s, 3.8%. The interobserver reproducibility of T2 measurements in the femoral cartilage was as follows: Z1d, 4.5%; Z1s, 2.3%; Z2d, 4.7%; and Z2s, 1.3%. The interobserver reproducibility of cartilage thickness measurements in the acetabular cartilage was as follows: Z1, 4.9%; Z2, 5.7%; and Z3, 6.5%. The interobserver reproducibility of cartilage thickness measurements in the femoral cartilage was 6.1% for Z1 and 6.6% for Z2.

Cartilage T2 under the unloaded condition did not show a predominant trend of differences between normal and dysplastic hips (Table 2). At zone Z1d of the acetabular cartilage, T2 values of the patients were significantly greater than those of the volunteers ($P$ = .01). Conversely, at zone Z1d of the femoral cartilage, T2 values of the patients were significantly lower than those of the volunteers ($P$ = .03).

In volunteers, there was no significant difference between T2 values under the unloaded condition and T2 values under the loaded condition at each ROI. In patients, T2 values with loading decreased significantly at acetabular cartilage zones Z1s and Z2s ($P$ = .02 and $P$ = .04, respectively). At acetabular cartilage zone Z1s, the decrease in T2 values with loading was significantly greater in patients with dysplasia than in healthy volunteers ($P$ = .04) (Table 2, Figs 3, 4).

With respect to cartilage thickness, the cartilage at most zones of the acetabular and femoral cartilage in dysplastic hips was significantly thicker than that in normal hips (Table 3). In volunteers, there was no significant difference between cartilage thickness under the unloaded condition and cartilage thickness under the loaded condition at each ROI. In patients, cartilage thickness with loading decreased significantly at acetabular cartilage zone Z1 ($P$ = .02). However, there were no significant differences in the changes in cartilage thickness between the volunteers and patients.

Among patients with hip dysplasia, results of Spearman correlation coefficient analysis showed an inverse correlation between patient age and T2 changes with loading at acetabular cartilage zone Z2d ($P$ = .04, $r$ = −0.52, Fig 5a) and at femoral cartilage zone Z1d ($P$ = .03, $r$ = −0.60, Fig 5b). Moreover, there was a positive correlation between center-edge angle and T2 changes with loading at acetabular cartilage zone Z1d ($P$ = .03, $r$ = 0.67, Fig 5c). There was no significant correlation between the T2 changes with loading and the body mass index of the patients at each ROI.

## Discussion

Normal hip joint biomechanics relating to pressure distribution on the articular cartilage and acetabular labrum have been studied extensively by using cadavers and computational-mathematical modeling (2,4,16,34,35). Konrath et al (34) measured the contact pressure between the acetabulum and femoral head of cadaveric hips by using a pressure-sensitive film and showed a tendency for a peripheral increase in load with maximal strength at the superior region of the normal acetabulum in a simulated single-limb stance. By using a computational simplified hip model, Chegini et al (16) showed an inverse correlation between the center-edge angle and the peak contact pressure with focal overloading of the lateral edge of the

**Table 2**

**T2 Value under Unloaded and Loaded Conditions and T2 Changes with Loading at Each Acetabular and Femoral Cartilage Zone**

| | T2 without Loading (msec) | | | T2 with Loading (msec) | | | T2 Change with Loading (%)† | | |
|---|---|---|---|---|---|---|---|---|---|
| Zone | Volunteers* | Patients* | *P* Value | Volunteers* | Patients* | *P* Value | Volunteers* | Patients* | *P* Value |
| Acetabular cartilage | | | | | | | | | |
| Z1d | 21.6 ± 2.7 | 25.4 ± 3.1 | .01‡ | 23.4 ± 4.1 | 25.2 ± 4.6 | .40 | 8.7 ± 14.6 | −0.7 ± 11.5 | .07 |
| Z1s | 32.8 ± 3.0 | 34.2 ± 5.4 | .53 | 33.0 ± 3.0 | 31.6 ± 6.2 | .53 | 1.2 ± 10.9 | −7.6 ± 10.6 | .04‡ |
| Z2d | 21.7 ± 3.0 | 24.5 ± 3.8 | .13 | 22.1 ± 3.6 | 25.5 ± 4.7 | .11 | 1.6 ± 6.9 | 4.4 ± 13.3 | .46 |
| Z2s | 33.3 ± 4.1 | 34.7 ± 4.0 | .42 | 32.1 ± 3.3 | 33.3 ± 3.3 | .39 | −3.2 ± 7.2 | −3.6 ± 6.7 | .93 |
| Z3d | 27.7 ± 6.9 | 25.8 ± 5.9 | .57 | 28.1 ± 7.2 | 25.9 ± 5.4 | .42 | 4.4 ± 26.9 | 1.2 ± 13.9 | .98 |
| Z3s | 39.8 ± 5.1 | 36.7 ± 6.4 | .22 | 39.0 ± 5.7 | 34.4 ± 4.8 | .04‡ | −1.3 ± 14.4 | −4.6 ± 14.8 | .53 |
| Femoral cartilage | | | | | | | | | |
| Z1d | 28.3 ± 3.5 | 25.0 ± 2.6 | .03‡ | 27.0 ± 3.7 | 26.6 ± 3.9 | .70 | −4.0 ± 11.9 | 6.5 ± 13.5 | .06 |
| Z1s | 36.1 ± 3.5 | 36.1 ± 4.3 | .74 | 36.7 ± 4.9 | 34.6 ± 4.4 | .39 | 1.9 ± 10.8 | −3.6 ± 12.6 | .33 |
| Z2d | 23.1 ± 4.5 | 27.8 ± 5.1 | .06 | 22.3 ± 3.0 | 27.9 ± 3.4 | .001‡ | −1.9 ± 13.7 | 2.1 ± 15.0 | .70 |
| Z2s | 34.1 ± 4.9 | 36.4 ± 5.5 | .13 | 33.6 ± 4.9 | 34.6 ± 5.7 | .57 | −1.0 ± 9.1 | −4.5 ± 9.8 | .39 |

* Data are given as means ± standard deviations.

† T2 change with loading was calculated for each volunteer or patient as follows: [(T2 value with loading − T2 value without loading)/T2 value without loading] × 100.

‡ The difference between the two groups was statistically significant.

acetabulum in dysplastic hips during simulated walking. There are large individual variations in the three-dimensional morphologic and material properties of the articular cartilage among patients with hip dysplasia (36). To our knowledge, there has been no biomechanical patient-specific analysis of patients with hip dysplasia reflecting morphologic and material diversions of the articular cartilage of individual patients.

MR imaging has the potential to help evaluate the load responsiveness of an articular cartilage. Rubenstein et al (17) observed a gradual decrease in the signal intensity of an excised bovine cartilage, beginning at the superficial cartilage layers and progressing to the overall depth of the cartilage with increasing pressure. A decrease in MR signal intensity with loading can be explained by extrusion of interstitial water and deformation of cartilage architecture within the cartilage (17,19). With use of high-spatial-resolution microscopic MR imaging, Alhadlaq and Xia (18) studied T2 changes in beagle cartilage specimens in response to external loading and found that the change in cartilage T2 showed a positive correlation with the strain value of compression.

**Figure 3**

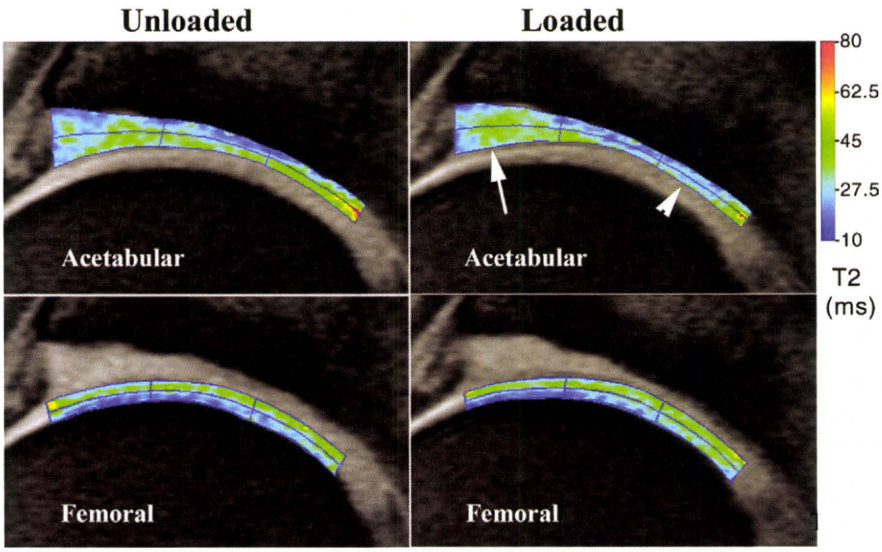


**Figure 3:** T2 maps of the acetabular and femoral cartilage on midcoronal MR images in a 30-year-old female volunteer. A low T2 is indicated by blue, and a high T2 is indicated by green or red. Under the loaded condition, the T2 of the acetabular cartilage was increased at the outer zones (Z1s and Z1d, arrow) and decreased at the inner, superficial zone (Z3s, arrowhead).

In the present study, we evaluated the change in cartilage T2 in the hip joint of living human subjects with loading. The topographic variation of cartilage T2, with higher T2 values at superficial zones in unloaded conditions, agrees with findings from a previous clinical study (37). The average T2 values with loading decreased at most superficial zones of the acetabular and femoral cartilages. This

**Table 3**

**Cartilage Thickness under Unloaded and Loaded Conditions and Changes in Thickness with Loading at Each Acetabular and Femoral Cartilage Zone**

| | Thickness without Loading (mm) | | | Thickness with Loading (mm) | | | Change in Thickness with Loading (%)† | | |
|---|---|---|---|---|---|---|---|---|---|
| Zone | Volunteers* | Patients* | *P* Value | Volunteers* | Patients* | *P* Value | Volunteers* | Patients* | *P* Value |
| Acetabular cartilage | | | | | | | | | |
| Z1 | 2.1 ± 0.7 | 2.4 ± 0.5 | .08 | 2.2 ± 0.7 | 2.2 ± 0.6 | .49 | 3.4 ± 12.9 | −7.9 ± 11.5 | .08 |
| Z2 | 1.6 ± 0.3 | 2.2 ± 0.5 | .001‡ | 1.6 ± 0.4 | 2.2 ± 0.4 | .004‡ | −2.6 ± 9.5 | −1.8 ± 9.4 | .74 |
| Z3 | 1.5 ± 0.3 | 1.9 ± 0.4 | .018‡ | 1.5 ± 0.2 | 1.9 ± 0.4 | .001‡ | −2.2 ± 14.0 | 2.6 ± 8.9 | .32 |
| Femoral cartilage | | | | | | | | | |
| Z1 | 1.2 ± 0.2 | 1.6 ± 0.3 | .001‡ | 1.2 ± 0.2 | 1.7 ± 0.4 | .008‡ | 4.5 ± 17.6 | 2.8 ± 15.8 | .61 |
| Z2 | 1.2 ± 0.2 | 1.8 ± 0.4 | .001‡ | 1.2 ± 0.3 | 1.8 ± 0.4 | .001‡ | −0.8 ± 15.2 | −0.4 ± 14.5 | .74 |

* Data are given as means ± standard deviations.

† Changes were calculated for each volunteer or patient as follows: (cartilage thickness with loading − cartilage thickness without loading)/cartilage thickness without loading × 100.

‡ The difference between the two groups was statistically significant.

**Figure 4**

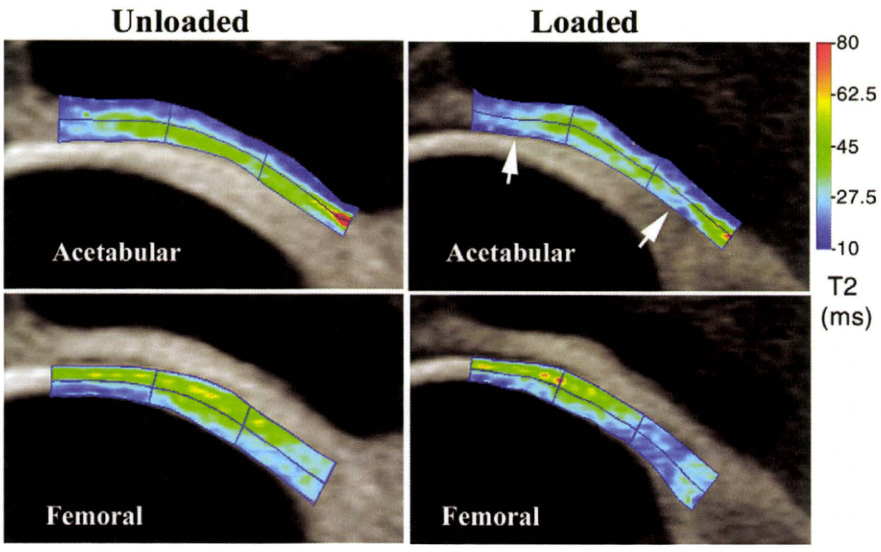


**Figure 4:** T2 maps of the acetabular and femoral cartilage on midcoronal MR images in a 28-year-old woman with hip dysplasia. Under the loaded condition, the T2 of the acetabular cartilage was decreased at both the outer and inner superficial zones (Z1s and Z3s, respectively, arrows).

finding was consistent with those from previous experimental studies (17,18). Although the mode of loading was different from that used in the present study, results of a clinical investigation evaluating cartilage T2 response to high-impact exercise with a cyclic compressive load showed a significant decrease in T2 values in the superficial femoral cartilage in the knee joints of healthy volunteers after 30 minutes of running (32). More important, we found that the decrease in T2 values at the outer superficial acetabular cartilage area with loading was significantly greater in dysplastic hips than in normal hips. Assuming that the decrease in T2 reflects changes in the solid matrix of the cartilage or interstitial water, our findings may indicate that dysplastic hips were subject to a substantial alteration in the extracellular matrix composition and/or fluid distribution at the outer acetabular cartilage when a load was applied.

Two underlying pathomechanisms may help explain this response. First, a decrease in T2 with loading might reflect a concentrated load-bearing force at the outer acetabular cartilage in dysplastic hips. This is supported by results of previous computational studies in which hip joint contact pressure was estimated (4,16) and the correlation between center-edge angle and T2 decrease with loading in our study. Second, a large T2 decrease in dysplastic hips with loading might indicate that the outer area of the acetabular cartilage was already involved in degenerative changes or injury and failed to appropriately adapt to the external compression force due to increased hydration and disorganized collagen structure within the cartilage. This assumption was partly supported by a significant increase in T2 at the outer acetabular cartilage in dysplastic hips, presumably in association with degenerative changes in the cartilage (38,39). Regardless of the possible mechanism, cartilage T2 mapping with loading presumably enabled the detection of a mechanically critical cartilage area where substantial changes in the ultrastructure or molecular composition of the cartilage occurred when a physiologic load was applied.

Patient age was inversely correlated with T2 changes at the deep zones of the acetabular and femoral cartilage

**Figure 5**

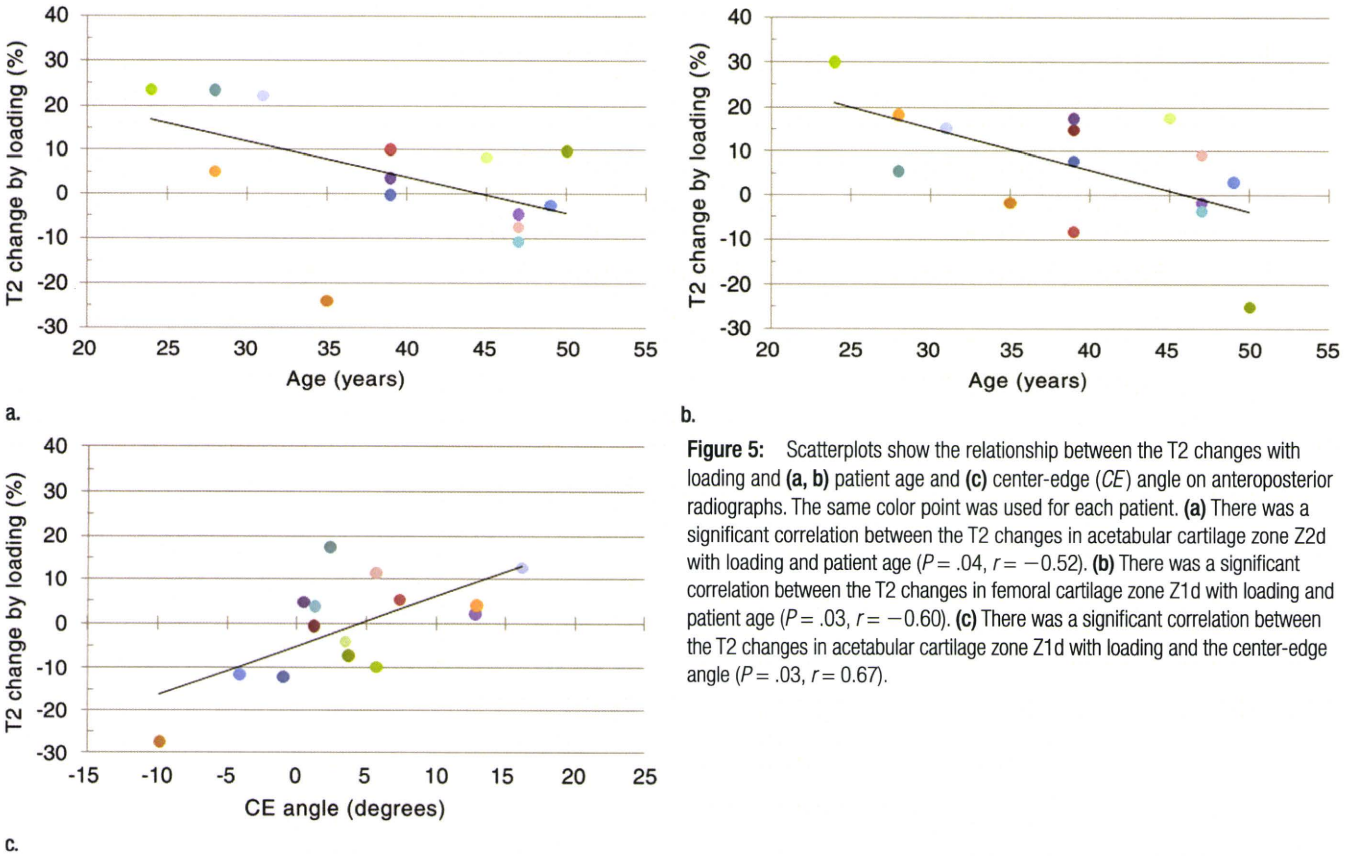


**Figure 5:** Scatterplots show the relationship between the T2 changes with loading and **(a, b)** patient age and **(c)** center-edge (*CE*) angle on anteroposterior radiographs. The same color point was used for each patient. **(a)** There was a significant correlation between the T2 changes in acetabular cartilage zone Z2d with loading and patient age ($P = .04$, $r = -0.52$). **(b)** There was a significant correlation between the T2 changes in femoral cartilage zone Z1d with loading and patient age ($P = .03$, $r = -0.60$). **(c)** There was a significant correlation between the T2 changes in acetabular cartilage zone Z1d with loading and the center-edge angle ($P = .03$, $r = 0.67$).

with loading. A previous experimental study in which compression force was applied on bone-cartilage plugs (17) showed a decrease of MR signal intensity in the superficial zone along with an increase of signal intensity in the deep zone at an initial pressure. These signal intensity changes were mainly accounted for by the depth-dependent movement of water content and deformation of the collagen architecture within the cartilage: With loading, interstitial water exudes from the cartilage surface or moves to a deeper zone of the cartilage, and this may contribute to the decrease of T2 in the superficial zone and the increase of T2 in the deep zone. With loading, originally parallel collagen fibers aligned perpendicular to the subchondral plate in the deep zone spread out and the portion of fibers oriented at the magic angle with respect to the static magnetic field increases; this may lead to an increase of cartilage T2 in the deep zone (40). With aging, however, permeability to fluid flow in the cartilage decreases (41) or cartilage stiffness increases in association with the accumulation of nonenzymatic glycation products (42), which may cause a depth-wise variation in T2 change with loading between younger and older patients.

T2 values calculated from two echoes were used for the evaluation of load responsiveness in cartilage T2. In many previous studies, T2 was calculated from images obtained with more than two echoes, and the initial echo image obtained with multiple-spin-echo imaging was excluded in the calculation of T2 to minimize T2 inaccuracy caused by stimulated echoes (32,33); however, the multiple-spin-echo sequence available in this study provided inferior image quality with lower in-plane resolution. A previous study in which a dual-spin-echo sequence was used for T2 assessment successfully achieved significant differences between the knee cartilages of healthy subjects and patients with osteoarthritis (38). Given the sufficiently high correlation to T2 values from multiple-spin-echo images in the present study, we consider T2 assessment with a dual-spin-echo sequence to provide a reliable assessment of the extracellular matrix in the hip cartilage. Although the present image acquisition sequence was not optimized for measuring cartilage thickness, most zones of the acetabular and femoral cartilage were significantly thicker in patients with dysplasia than in healthy volunteers. This finding was consistent with that from a previous study that used MR imaging with fat-suppressed three-dimensional fast spoiled gradient-echo sequences (43). In our study, however, evaluation of cartilage thickness with loading did not enable the detection of a difference in response to loading between healthy volunteers and patients with hip dysplasia.

MR imaging under the loaded condition was examined previously in patients with an upright posture in the evaluation of the cartilage contact area in the knee or impingement between the femoral neck and the acetabular rim in the hip by using open-configuration MR units (44,45). The image quality obtained with open-configuration MR units is relatively low owing to the low magnetic field strength (0.5 T), and MR images obtained with patients in an upright position are more susceptible to motion artifacts. We assumed that the use of a closed-bore MR unit with a high field strength (3.0 T) and the application of a mechanical loading device with the patient in a supine posture were suitable for assessing cartilage microstructural properties with loading because a high image resolution can be acquired with a sufficient signal-to-noise ratio. In a previous investigation in which a similar mechanical device was used, compressive loading at T2 mapping of knee cartilage was successfully evaluated (46). However, it is unclear how accurately this system simulated the mechanical environment in the physiologic standing position because it did not incorporate surrounding muscle action such as contraction of the iliopsoas, gluteus maximus, and gluteus medius muscles and the relative angular and rotational position of the pelvis against the femoral head might be different.

This study had several limitations. First, cartilage T2 was assessed only on midcoronal hip joint images, and anterior or posterior areas of the acetabular and femoral cartilage were not evaluated because the extensively curved joint surface is susceptible to partial volume averaging. Additional investigations with various imaging planes are necessary to clarify load responsiveness over the entire articular cartilage. Second, delineation of the cartilage surface in ROI placement may be difficult owing to the close contact between the acetabular and femoral cartilages—particularly under the loaded condition. Furthermore, T2 assessment of most superficial cartilage areas is also susceptible to partial volume averaging with synovial fluid on the midcoronal images, and this might be accentuated with the use of relatively thick sections (5 mm). By referring to the corresponding images obtained with a longer echo time, we were careful not to include joint fluid in the ROIs. However, to diminish these inherent difficulties in delineating the cartilage surface and to decrease the susceptibility of the hip joint to partial volume artifacts, further improvement is necessary so that images can be acquired with a higher spatial resolution and a sufficient signal-to-noise ratio. Third, dysplastic hips at both the prearthritic and early arthritic stage were examined in this study. Because hips with radiologic findings of osteoarthritis have a high incidence of cartilage abnormalities (39,47), the responsiveness of cartilage T2 to loading may be partly influenced by the underlying cartilage degeneration in hip dysplasia. Because of the small number of patients in this study, the load responsiveness of cartilage T2 was not compared between patients at a prearthritic stage and those at an early arthritic stage, and further investigations with a larger number of patients are needed to explore the influence of the radiologic osteoarthritis stage on the response of cartilage T2 to loading. Fourth, the response of cartilage thickness and T2 to loading was evaluated after preloading for an average of 6 minutes, followed by loading for 13.5 minutes during MR imaging. Herberhold et al (48) studied the deformational behavior of the articular cartilage during static loading of 150% of the body weight with femoropatellar knee imaging ex vivo; the deformations of the patellar and femoral cartilages after 8 minutes of compression were 25%–30% of the final deformations of those cartilages after 214 minutes of compression. It was unknown whether deformational equilibrium of the articular cartilage was achieved after preloading for an average of 6 minutes in this study. Although the location of the cartilage and magnitude of compression force used in our study differed from those used by Herberhold et al (48), our results may represent a relatively early response of the hip cartilage under static loading, simulating the status of the articular cartilage in the standing position for a relatively short period. In addition, the numbers of volunteers and patients were small. Because this was, to our knowledge, the first investigation to compare loaded cartilage T2 mapping in patients with hip dysplasia and healthy volunteers, we were not able to perform power analysis for a sufficient number of subjects before the start of the study. However, because we observed a significant difference in the T2 response of cartilage to loading between the patients and volunteers, we believe that loaded cartilage T2 mapping may help detect mechanically critical cartilage areas in patients with hip dysplasia. The volunteers were significantly younger than the patients. Previous reports have indicated that the T2 of the knee joint is significantly affected by age (33). Although the relationship between age and the T2 of cartilage in the hip joint was not clarified, the significant differences in T2 with unloading and T2 changes with loading between the volunteers and patients could have been partly influenced by the relatively large age difference between the groups. Additional studies are required to compare the response of cartilage T2 to loading between age-matched volunteers and patients.

In conclusion, the decrease of cartilage T2 at the outer superficial zones of the acetabular cartilage with loading was significantly greater in patients with hip dysplasia than in healthy volunteers. This site-specific change in cartilage T2 with loading presumably represents a mechanically critical response in which substantial changes occur in the ultrastructure or molecular composition of the cartilage. Additional follow-up studies are needed to clarify the potential of using T2 changes with loading to predict the subsequent progression of osteoarthritis.

## References

1. Harris WH. Etiology of osteoarthritis of the hip. Clin Orthop Relat Res 1986;(213):20–33.

2. Michaeli DA, Murphy SB, Hipp JA. Comparison of predicted and measured contact pressures in normal and dysplastic hips. Med Eng Phys 1997;19(2):180–186.

3. Hadley NA, Brown TD, Weinstein SL. The effects of contact pressure elevations and aseptic necrosis on the long-term outcome of congenital hip dislocation. J Orthop Res 1990;8(4):504–513.

4. Hipp JA, Sugano N, Millis MB, Murphy SB. Planning acetabular redirection osteotomies based on joint contact pressures. Clin Orthop Relat Res 1999;(364):134–143.

5. Genda E, Iwasaki N, Li G, MacWilliams BA, Barrance PJ, Chao EY. Normal hip joint contact pressure distribution in single-leg standing: effect of gender and anatomic parameters. J Biomech 2001;34(7):895–905.

6. Anwar MM, Sugano N, Matsui M, Takaoka K, Ono K. Dome osteotomy of the pelvis for osteoarthritis secondary to hip dysplasia: an over five-year follow-up study. J Bone Joint Surg Br 1993;75(2):222–227.

7. Zhang W, Moskowitz RW, Nuki G, et al. OARSI recommendations for the management of hip and knee osteoarthritis. II. OARSI evidence-based, expert consensus guidelines. Osteoarthritis Cartilage 2008;16(2):137–162.

8. Lane NE, Lin P, Christiansen L, et al. Association of mild acetabular dysplasia with an increased risk of incident hip osteoarthritis in elderly white women: the study of osteoporotic fractures. Arthritis Rheum 2000;43(2):400–404.

9. Reijman M, Hazes JM, Pols HA, Koes BW, Bierma-Zeinstra SM. Acetabular dysplasia predicts incident osteoarthritis of the hip: the Rotterdam study. Arthritis Rheum 2005;52(3):787–793.

10. Delaunay S, Dussault RG, Kaplan PA, Alford BA. Radiographic measurements of dysplastic adult hips. Skeletal Radiol 1997;26(2):75–81.

11. Day WH, Swanson SA, Freeman MA. Contact pressures in the loaded human cadaver hip. J Bone Joint Surg Br 1975;57(3):302–313.

12. Genda E, Konishi N, Hasegawa Y, Miura T. A computer simulation study of normal and abnormal hip joint contact pressure. Arch Orthop Trauma Surg 1995;114(4):202–206.

13. Ferguson SJ, Bryant JT, Ganz R, Ito K. The influence of the acetabular labrum on hip joint cartilage consolidation: a poroelastic finite element model. J Biomech 2000;33(8):953–960.

14. Rapperport DJ, Carter DR, Schurman DJ. Contact finite element stress analysis of the hip joint. J Orthop Res 1985;3(4):435–446.

15. Wang Y, Wei HW, Yu TC, Cheng CK. Parametric analysis of the stress distribution on the articular cartilage and subchondral bone. Biomed Mater Eng 2007;17(4):241–247.

16. Chegini S, Beck M, Ferguson SJ. The effects of impingement and dysplasia on stress distributions in the hip joint during sitting and walking: a finite element analysis. J Orthop Res 2009;27(2):195–201.

17. Rubenstein JD, Kim JK, Henkelman RM. Effects of compression and recovery on bovine articular cartilage: appearance on MR images. Radiology 1996;201(3):843–850.

18. Alhadlaq HA, Xia Y. The structural adaptations in compressed articular cartilage by microscopic MRI (microMRI) T(2) anisotropy. Osteoarthritis Cartilage 2004;12(11):887–894.

19. Liess C, Lüsse S, Karger N, Heller M, Glüer CC. Detection of changes in cartilage water content using MRI T2-mapping in vivo. Osteoarthritis Cartilage 2002;10(12):907–913.

20. Burstein D, Gray ML. Is MRI fulfilling its promise for molecular imaging of cartilage in arthritis? Osteoarthritis Cartilage 2006;14(11):1087–1090.

21. Link TM, Stahl R, Woertler K. Cartilage imaging: motivation, techniques, current and future significance. Eur Radiol 2007;17(5):1135–1146.

22. Eckstein F, Burstein D, Link TM. Quantitative MRI of cartilage and bone: degenerative changes in osteoarthritis. NMR Biomed 2006;19(7):822–854.

23. Nieminen MT, Töyräs J, Rieppo J, et al. Quantitative MR microscopy of enzymatically degraded articular cartilage. Magn Reson Med 2000;43(5):676–681.

24. Lüsse S, Claassen H, Gehrke T, et al. Evaluation of water content by spatially resolved transverse relaxation times of human articular cartilage. Magn Reson Imaging 2000;18(4):423–430.

25. Inoue K, Wicart P, Kawasaki T, et al. Prevalence of hip osteoarthritis and acetabular dysplasia in French and Japanese adults. Rheumatology (Oxford) 2000;39(7):745–748.

26. Mosher TJ, Collins CM, Smith HE, et al. Effect of gender on in vivo cartilage magnetic resonance imaging T2 mapping. J Magn Reson Imaging 2004;19(3):323–328.

27. Fredensborg N. The CE angle of normal hips. Acta Orthop Scand 1976;47(4):403–405.

28. Crowe JF, Mani VJ, Ranawat CS. Total hip replacement in congenital dislocation and dysplasia of the hip. J Bone Joint Surg Am 1979;61(1):15–23.

29. Kellgren JH, Lawrence JS. Radiological assessment of osteo-arthrosis. Ann Rheum Dis 1957;16(4):494–502.

30. Reijman M, Hazes JM, Pols HA, Bernsen RM, Koes BW, Bierma-Zeinstra SM. Validity and reliability of three definitions of hip osteoarthritis: cross sectional and longitudinal approach. Ann Rheum Dis 2004;63(11):1427–1433.

31. Bellamy N, Buchanan WW, Goldsmith CH, Campbell J, Stitt LW. Validation study of WOMAC: a health status instrument for measuring clinically important patient relevant outcomes to antirheumatic drug therapy in patients with osteoarthritis of the hip or knee. J Rheumatol 1988;15(12):1833–1840.

32. Mosher TJ, Smith HE, Collins C, et al. Change in knee cartilage T2 at MR imaging after running: a feasibility study. Radiology 2005;234(1):245–249.

33. Mosher TJ, Dardzinski BJ, Smith MB. Human articular cartilage: influence of aging and early symptomatic degeneration on the spatial variation of T2—preliminary findings at 3 T. Radiology 2000;214(1):259–266.

34. Konrath GA, Hamel AJ, Olson SA, Bay B, Sharkey NA. The role of the acetabular labrum and the transverse acetabular ligament in load transmission in the hip. J Bone Joint Surg Am 1998;80(12):1781–1788.

35. von Eisenhart R, Adam C, Steinlechner M, Müller-Gerbl M, Eckstein F. Quantitative determination of joint incongruity and pressure distribution during simulated gait and cartilage thickness in the human hip joint. J Orthop Res 1999;17(4):532–539.

36. Noble PC, Kamaric E, Sugano N, et al. Three-dimensional shape of the dysplastic femur: implications for THR. Clin Orthop Relat Res 2003;(417):27–40.

37. Watanabe A, Boesch C, Siebenrock K, Obata T, Anderson SE. T2 mapping of hip articular cartilage in healthy volunteers at 3T: a study of topographic variation. J Magn Reson Imaging 2007;26(1):165–171.

38. Dunn TC, Lu Y, Jin H, Ries MD, Majumdar S. T2 relaxation time of cartilage at MR imaging: comparison with severity of knee osteoarthritis. Radiology 2004;232(2):592–598.

39. Nishii T, Tanaka H, Sugano N, Sakai T, Hananouchi T, Yoshikawa H. Evaluation of cartilage matrix disorders by T2 relaxation time in patients with hip dysplasia. Osteoarthritis Cartilage 2008;16(2):227–233.

40. Gründer W, Kanowski M, Wagner M, Werner A. Visualization of pressure distribution within loaded joint cartilage by application of angle-sensitive NMR microscopy. Magn Reson Med 2000;43(6):884–891.

41. Grushko G, Schneiderman R, Maroudas A. Some biochemical and biophysical parameters for the study of the pathogenesis of osteoarthritis: a comparison between the processes of ageing and degeneration in human hip cartilage. Connect Tissue Res 1989;19(2-4):149–176.

42. Bank RA, Bayliss MT, Lafeber FP, Maroudas A, Tekoppele JM. Ageing and zonal variation in post-translational modification of collagen in normal human articular cartilage: the age-related increase in non-enzymatic glycation affects biomechanical properties of cartilage. Biochem J 1998; 330(pt 1):345–351.

43. Nishii T, Sugano N, Sato Y, Tanaka H, Miki H, Yoshikawa H. Three-dimensional distribution of acetabular cartilage thickness in patients with hip dysplasia: a fully automated computational analysis of MR imaging. Osteoarthritis Cartilage 2004;12(8):650–657.

44. Gold GE, Besier TF, Draper CE, Asakawa DS, Delp SL, Beaupre GS. Weight-bearing MRI of patellofemoral joint cartilage contact area. J Magn Reson Imaging 2004;20(3):526–530.

45. Yamamura M, Miki H, Nakamura N, Murai M, Yoshikawa H, Sugano N. Open-acetabular impingement. J Orthop Res 2007;25(12): 1582–1588.

46. Nishii T, Kuroda K, Matsuoka Y, Sahara T, Yoshikawa H. Change in knee cartilage T2 in response to mechanical loading. J Magn Reson Imaging 2008;28(1):175–180.

47. Noguchi Y, Miura H, Takasugi S, Iwamoto Y. Cartilage and labrum degeneration in the dysplastic hip generally originates in the anterosuperior weight-bearing area: an arthroscopic observation. Arthroscopy 1999;15(5):496–506.

48. Herberhold C, Faber S, Stammberger T, et al. In situ measurement of articular cartilage deformation in intact femoropatellar joints under static loading. J Biomech 1999;32(12):1287–1295.

Osteoarthritis and Cartilage 18 (2010) 902–908

Osteoarthritis and Cartilage

# Loading and knee alignment have significant influence on cartilage MRI T2 in porcine knee joints

T. Shiomi †, T. Nishii †‡*, H. Tanaka §, Y. Yamazaki ||, K. Murase ||, A. Myoui †¶, H. Yoshikawa †, N. Sugano †‡

† *Department of Orthopaedic Surgery, Osaka University Medical School, Osaka, Japan*
‡ *Department of Orthopaedic Medical Engineering, Osaka University Medical School, Osaka, Japan*
§ *Department of Radiology, Osaka University Medical School, Osaka, Japan*
|| *Department of Medical Physics and Engineering, Osaka University Medical School, Osaka, Japan*
¶ *Medical Center for Translational Research, Osaka University Hospital, Osaka, Japan*

ARTICLE INFO

*Article history:*
Received 14 October 2009
Accepted 3 May 2010

*Keywords:*
MRI
Cartilage
T2
Static loading
Knee alignment

SUMMARY

*Objective:* Physiological magnetic resonance imaging (MRI) under loading or knee malalignment conditions has not been thoroughly investigated. We assessed the influence of static loading and knee alignment on T2 (transverse relaxation time) mapping of the knee femoral cartilage of porcine knee joints using a non-metallic pressure device.

*Methods:* Ten porcine knee joints were harvested *en bloc* with intact capsules and surrounding muscles and imaged using a custom-made pressure device and 3.0-T MRI system. Sagittal T2 maps were obtained (1) at knee neutral alignment without external loading (no loading), (2) under mechanical compression of 140 N (neutral loading), and (3) under the same loading conditions as in (2) with the knee at 10° varus alignment (varus loading). T2 values of deep, intermediate, and superficial zones of the medial and lateral femoral cartilages at the weight-bearing area were compared among these conditions using custom-made software. Cartilage contact pressure between the femoral and tibial cartilages, measured by a pressure-sensitive film, was correlated with cartilage T2 measurements.

*Results:* In the medial cartilage, mean T2 values of the deep, intermediate, and superficial zones decreased by 1.4%, 13.0%, and 6.0% under neutral loading. They further decreased by 4.3%, 19.3%, and 17.2% under varus loading compared to no loading. In the lateral cartilage, these mean T2 values decreased by 3.9%, 7.7%, and 4.2% under neutral loading, but increased by 1.6%, 9.6%, and 7.2% under varus loading. There was a significant decrease in T2 values in the intermediate zone of the medial cartilage under both neutral and varus loading, and in the superficial zone of the medial cartilage under varus loading ($P < 0.05$). Total contact pressure values under neutral loading and varus loading conditions significantly correlated with T2 values in the superficial and intermediate zones of the medial cartilages.

*Conclusions:* The response of T2 to change in static loading or alignment varied between the medial and lateral cartilages, and among the deep, intermediate, and superficial zones. These T2 changes were significantly related to the contact pressure measurements. Our results indicate that T2 mapping under loading allows non-invasive, biomechanical assessment of site-specific stress distribution in the cartilage.



## Introduction

Knee imaging using quantitative magnetic resonance imaging (MRI) techniques such as delayed gadolinium-enhanced MRI of cartilage (dGEMRIC), transverse relaxation time (T2) mapping and T1rho showed great advancements in non-invasive assessment of the articular cartilage, particularly with regard to matrix composition and degenerative changes[1–4]. Sensitive evaluations of water, collagen, and proteoglycan content or collagen arrangement in the cartilage *in vivo* were made using the aforementioned techniques, without performing destructive retrieval analysis. Quantitative MRI revealed site-specific and age- or sex-dependent variation in normal cartilage composition and allowed early detection of osteoarthritic involvement of knee cartilages[3,5]. MRI in most of these investigations was performed without externally loading the knee with patients or volunteers lying supine on the imaging table.

The articular cartilage in the knee joint has a load-bearing function in conjunction with the interposed meniscus owing to its highly organized collagen architecture and the osmotic pressure

* Address correspondence and reprint requests to: Takashi Nishii, Department of Orthopaedic Medical Engineering, Osaka University Medical School, 2-2 Yamadaoka, Suita, Osaka 565-0871, Japan. Tel: 81-6-6879-3271; Fax: 81-6-6879-3272.
*E-mail address:* nishii@ort.med.osaka-u.ac.jp (T. Nishii).

1063-4584/$ – see front matter © 2010 Osteoarthritis Research Society International. Published by Elsevier Ltd. All rights reserved.
doi:10.1016/j.joca.2010.05.002

due to proteoglycan and interstitial water. While performing daily activities such as standing or walking, the articular cartilage in the knee joint is subjected to substantial external loading, which leads to cartilage deformation along with alteration in the collagen architecture or water distribution within the cartilage[6,7]. This property of the cartilage under loading differs among individuals, depending upon factors such as weight, knee alignment, ligament instability, and involvement of injury or degeneration of the cartilage and meniscus. Therefore, it is important to evaluate the articular cartilage under loading for each individual to understand the physiological and biomechanical status of the knee and to explore the disorders of stress resistance function of the cartilage that may lead to progression of osteoarthritis.

Responsiveness of the normal cartilage to compressive loading was investigated using excised cartilage plugs or exposed articular surfaces in experimental studies on MRI[8–10]. Changes in cartilage thickness and signal intensity were observed in response to an increase in loading. Among all MRI parameters, cartilage T2 mapping of cartilage is influenced by water content and collagen fiber orientation of cartilage and is indicated as a potent quantitative index for the load response of the articular cartilage[11–13]. However, few studies have investigated the load response of the articular cartilage in an intact knee joint, with preservation of the other fundamental structures such as menisci, ligaments, and capsules.

We developed a non-metallic pressure device for intact porcine knee joints that allowed MRI under variable loading or knee alignment conditions as a whole-joint model retaining the menisci, ligaments, and capsules *in situ*. The purpose of this study was to assess the load-bearing function of the femoral cartilage in association with knee alignment, using cartilage T2 as a surrogate of cartilage matrix changes.

## Materials and methods

### *Preparation of porcine specimens and loading device*

Ten fresh porcine knee joints were harvested *en bloc* with intact capsules and surrounding muscles and stored at −40°C. On the day of MRI, specimens were thawed at room temperature before the investigation. After conducting imaging and mechanical experiments, macroscopic inspection of the joint surfaces did not reveal any signs of joint disease or cartilage degeneration in the specimens used.

Knee joints were mounted in the non-metallic custom compression device, which was fitted into the head coil (eight-channel brain phased array coil, GE Healthcare, WI, USA) of an MRI scanner (Fig. 1). The femoral shaft was firmly fixed to the non-mobile base of the device by holding it between two acryl blades. The tibia was firmly fixed to the opposite side of the mobile plate such that tibial movement along the longitudinal axis and varus/valgus rotation of the knee was possible. The knee was positioned at 20° flexion, simulating the normal standing position of pigs. Under static loading conditions, axial compression force was transmitted to the knee joint *via* a sliding plate bounded by a foam material. The load was generated by a screw compression driver on one end. The viscoelastic foam material, which was made of polyolefin elastomer (Fig. 1), was compressed by 10 mm displacement and the uniaxial constitution force according to the degree of displacement was transmitted to the knee joint through an acryl plate. We used new foam material on each knee joint to avoid degeneration of the foam material. Hayashi *et al.* studied static and dynamic characteristics and stability of some kinds of elastomeric polymers by uniaxial tensile and fatigue tests in air, and demonstrated polyolefin elastomer had little stress relaxation[14]. The compression force was applied to achieve 140 N across the tibiofemoral joint, which corresponded to approximately one-third of the body weight of the specimen.

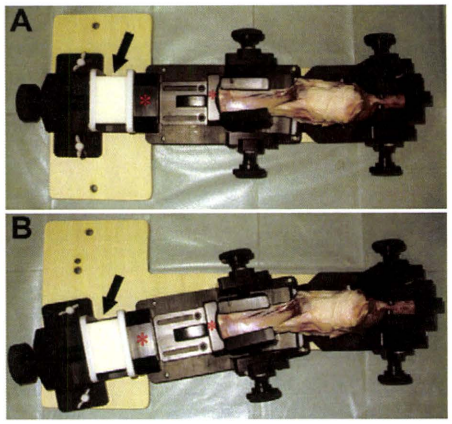


**Fig. 1.** Custom-made compression device along with a porcine knee joint. Axial compression force was transmitted to the knee joint *via* a sliding plate (*) bounded by a viscoelastic foam material (arrow). A: neutral position. B: 10° varus position.

### *Accuracy test of loading in custom compression device*

In a preliminary test, loading force in the custom compression device was measured using an incompressible testing rod equipped with a load cell (TU-BR, TEAC, Japan). The accuracy of the load cell is within 0.05% rated output in non-linearity which means accuracy of linear output, and within 0.05% rated output in hysteresis which means reproducibility during loading. Compression force equivalent to 140 N was applied continuously, and real force across the testing rod was recorded from the load cell after 5, 10 and 30 min of compression to determine the time course of change in force measurements. This test was repeated five times, and the mean force measurements and the values of coefficient of variation [standard deviation/mean × 100 (%)] were 140 N and 1.5% at 5 min, 138 N and 1.5% at 10 min, and 134 N and 1.8% at 30 min. We confirmed that constant pressure was applied after 5 min–30 min of compression by the loading device.

### *MRI*

MRI was performed using a 3.0-T MRI system (GE Healthcare). The device was placed in a head-first orientation in the center of the head coil. First, sagittal T2 maps and three-dimensional (3D) spoiled gradient-echo (SPGR) images were obtained for the lateral and medial femorotibial joints with neutral knee alignment and no external compression (no loading). Next, sagittal T2 maps and 3D SPGR images were obtained after 5 min of compression (neutral loading-1). After imaging at neutral loading-1, compression was continued for 30 min. Sagittal T2 maps and 3D SPGR images were obtained again after 30 min of compression (neutral loading-2) to examine the influence of loading duration on cartilage T2 measurements compared with neutral loading-1. Finally, sagittal T2 maps and 3D SPGR images were obtained under the same compression conditions as above with the knee at 10° varus alignment (varus loading).

T2 maps were generated using a monoexponential fit from two-dimensional (2D) multi-spin echo sequences (TR, 1500 ms; eight echoes between 10.0 ms and 80.0 ms; field of view, 10 cm; matrix, 384 × 256; slice thickness, 3 mm; signal averaging, 1; acquiring time, 6 min and 51 s). Frequency encoding was oriented in the cranial-to-caudal direction. 3D SPGR images were acquired with fat suppression (TR, 50 ms; TE, 10 ms; field of view, 10 cm; matrix, 512 × 256; slice thickness, 3 mm; signal averaging, 4; acquiring

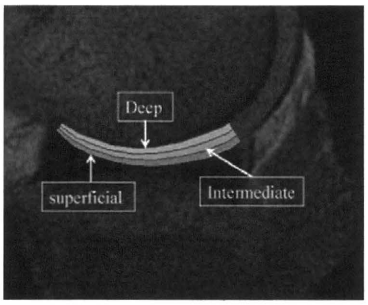


**Fig. 2.** Sagittal view of the femoral cartilage in the porcine knee, which was subdivided into three zones using custom-made software.

time, 2 min and 35 s). In both sequences, the same sagittal imaging planes were obtained in each examination series using identical axial localizing images.

*Image analysis*

Data was analyzed using custom-made software (Baum version 1.00; Osaka university, Japan). Sagittal images passing through the middle of the medial and lateral femoral condyles were used. The region of interest (ROI) was manually defined on the weight-bearing area of the medial and lateral femoral cartilages between the anterior and posterior margins of the meniscus based on SPGR images. The ROI was then transferred to the corresponding T2 maps and subdivided into superficial, intermediate, and deep zones with thickness one-third that of the total cartilage, automatically yielding mean T2 values of each subdivided ROI (Fig. 2). Definitions of ROI were repeated twice by a single observer (TS) and the T2 values of each medial and lateral ROI were averaged. Reproducibility between the two measurements was calculated as the coefficient of variation and mean reproducibility were calculated as the root mean square average for all specimens. Reproducibility values of T2 measurements in the superficial, intermediate, and deep zones were 3%, 4%, and 3% in the medial cartilage and 5%, 3%, and 4% in the lateral cartilage, respectively. Inter-observer reproducibility between two observers (TS and IN, an orthopaedic surgeon) for definition of ROI was also evaluated in five knee joints. The reproducibility of T2 measurements in the superficial, intermediate, and deep zones were 5%, 4%, and 5% in the medial cartilage and 4%, 3%, and 3% in the lateral cartilage, respectively.

*Joint pressure analysis with pressure-sensitive film*

Following MRI, the knee joints were wrapped in gauze soaked in phosphate buffered saline (PBS) solution to be kept moist, and left for 10 h in an unloaded condition at 20°C in the acryl box. Two pieces of pressure-sensitive film (FUJI PRESCALE low sensitivity, FUJIFILM, Japan) were placed between the femur and the meniscus on the medial and lateral sides after making a small opening in the capsule. The incisions allowed access to the posterior root of the lateral or medial meniscus and facilitated inspection of the posterior compartments to confirm consistent placement of the film below the lateral and medial femoral condyle as well as to verify that the film was not folded on itself. Just as in MRI examinations, the joints were mounted in the custom compression device. Neutral loading-1 was applied for the corresponding imaging time. Films were removed, calibrated with a 0.5 $cm^2$ stamp in a material-testing machine by applying a set of defined loads, and the staining of the film converted into pressure intervals (N) with image analysis. The same pressure analysis was conducted for varus loading. Fukubayashi *et al.* estimated accuracy of Fuji Prescale films within 10%–15%[15], and Wu *et al.* reported the measurement error of the film was approximately 10%[16].

*Statistical analysis*

T2 values under no loading, neutral loading-1, neutral loading-2, and varus loading conditions at each ROI were compared using a paired *t*-test to estimate the influence of varying compression and knee alignment. Relationships among T2 values in each zone and joint pressure measurements recorded by a pressure-sensitive film were evaluated using Spearman's correlation coefficient. $P < 0.05$ was considered significant.

## Results

Under no loading, mean T2 values of the deep, intermediate, and superficial zones were 59.3 ± 3.7 ms, 62.4 ± 7.6 ms, and 67.3 ± 6.4 ms in the medial cartilage, and 62.6 ± 7.5 ms, 64.6 ± 9.2 ms, 71.9 ± 7.8 ms in the lateral cartilage (Table I), respectively. T2 values in the medial and lateral superficial zones had significantly higher values compared to medial and lateral deep zones ($P < 0.05$).

In the medial cartilage, mean T2 values of the deep, intermediate, and superficial zones decreased by 1.4%, 13.0%, and 6.0% under neutral loading-1, and further decreased by 4.3%, 19.3%, and 17.2% under varus loading, compared with the mean T2 values under no loading (Figs. 3 and 4). In the lateral cartilage, these T2 values decreased by 3.9%, 7.7%, and 4.2% under neutral loading-1, but increased by 1.6%, 9.6%, and 7.2% under varus loading (Figs. 3 and 5). There was a significant decrease in T2 values in the intermediate zone of the medial cartilage under both neutral loading-1 and varus loading ($P < 0.05$). In all three zones, changes in T2 time between neutral loading-1 and neutral loading-2 ranged from 0.8% to 3.7%, but the difference was not significant (Table II).

**Table I**
T2 values in each zone under no loading and each loading condition ($N = 10$)

| | No loading | Neutral loading-1 | | | Varus loading | | |
|---|---|---|---|---|---|---|---|
| | Mean T2 (SD) | Mean T2 (SD) | Change (95% CI) | *P*-Value | Mean T2 (SD) | Change (95% CI) | *P*-Value |
| Medial cartilage | | | | | | | |
| Deep | 59.3 (3.7) | 58.4 (5.2) | −1.4 (−5.7, 2.9) | 0.68 | 54.9 (5.2) | −4.3 (−7.3, −1.4) | 0.14 |
| Intermediate | 62.4 (7.6) | 54.4 (7.4) | −13.0 (−17.3, −8.7) | 0.03* | 46.7 (9.1) | −19.3 (−23.9, −14.6) | 0.0005* |
| Superficial | 67.3 (6.4) | 63.1 (6.4) | −6.0 (−9.1, −3.0) | 0.17 | 53.4 (5.1) | −17.2 (−19.1, −15.4) | <0.0001* |
| Lateral cartilage | | | | | | | |
| Deep | 62.6 (7.5) | 60.2 (6.1) | −3.9 (−8.0, 0.3) | 0.44 | 63.7 (6.5) | 1.6 (−2.8, 6.1) | 0.75 |
| Intermediate | 64.6 (9.2) | 59.6 (8.4) | −7.7 (−10.5, −4.9) | 0.22 | 70.7 (5.6) | 9.6 (3.5, 15.6) | 0.09 |
| Superficial | 71.9 (7.8) | 68.8 (9.0) | −4.2 (−7.5, −1.0) | 0.43 | 77.1 (8.5) | 7.2 (3.9, 10.5) | 0.17 |

Changes were calculated as (values at each loading condition − values at no loading)/values at no loading × 100.
95% CI: confidence interval.
* Significant difference between values under no loading and each loading condition.

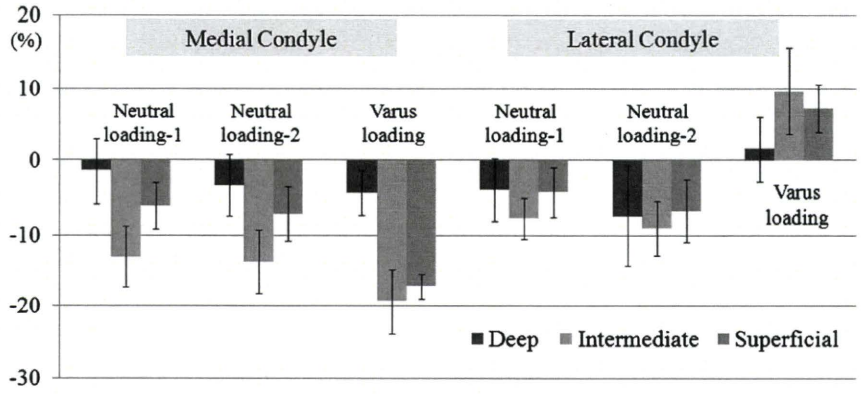


**Fig. 3.** Change in T2 values (95% confidence interval error bars) at each loading condition. ($N = 10$) Changes were calculated as (values at each loading condition – values at no loading)/values at no loading × 100.

Total contact pressure values at the medial and lateral femoral cartilages were $47 \pm 8.4$ N and $46 \pm 5.1$ N under neutral loading-1 and $94 \pm 21$ N and $35 \pm 7.8$ N under varus loading (Fig. 6). These values significantly correlated with T2 values in the intermediate (neutral loading-1 and varus loading: $r = -0.64$ and $-0.49$) and superficial ($r = -0.48$ and $-0.55$) zones of the medial cartilage, and in the intermediate ($r = -0.48$ and $-0.78$) and superficial (varus loading: $r = -0.73$) zones of the lateral cartilage (Table III, Fig. 7).

## Discussion

Changes in signal intensity and quantitative assessments of MRI in response to static loading were investigated using bone–cartilage plugs in experimental studies[8,9,11,17]. Rubenstein *et al.* examined the MRI appearance of an excised bovine cartilage under static compression[9]. At an initial pressure of 1.10 MPa, they observed a decrease in signal intensity in the thin superficial zone of the cartilage but an increase in the deep zone. This was followed by a gradual decrease in signal intensity along the entire depth of the cartilage as the pressure was increased. At a continuous pressure of 0.69 MPa, using a pressure cell, Kaufman *et al.* observed a reduction in T1 and T2 values in both normal and trypsin-degraded bovine cartilage discs under static pressure[11]. They calculated the permeability of the cartilage as a function of cartilage strain, and showed that the high permeability seen in the uncompressed state decreased progressively with increasing strain. A decrease in T2 values under static loading has been mainly accounted for depth-dependent movement of water content and deformation of the collagen architecture within the cartilage[9,13,18,19]. Approximately 80% of a normal cartilage is water[20], and 94% of this water is freely diffusible and readily exchanges with the intraarticular synovial fluid[21]. On applying static compression onto the cartilage, interstitial water exudes from the cartilage surface or moves to a deeper zone of the cartilage, contributing to depth-specific changes in signal intensity of T2 on MRI[22]. Furthermore, T2 of the articular cartilage is subject to the "magic angle effect" in accordance with the relative position between collagen alignment in the cartilage and direction of the external magnetic field[23]. T2 would change under loading because of altered orientation of collagen fibers relative to the external magnetic field, but the effect of the change is influenced by pressure distribution and original anisotropic collagen fiber architecture along its depth[22]. Reiter *et al.* investigated water compartmentation in cartilage using multiexponential analysis of T2 relaxation data to evaluate anisotropy in the cartilage[24]. Hardy *et al.* demonstrated elastographic method for measuring the spatial variation of compression within articular cartilage[25].

In the present study, the influence of static loading on T2 mapping of the cartilage was investigated using whole animal knee joints retaining all intraarticular structures, capsules, and surrounding muscles. These realistic joint models allowed for static loading under near-physiological conditions unlike excised cartilage specimens, and permitted examining simulated disease conditions (e.g., varus knee alignment). As expected from experimental studies[8,11], a decrease in cartilage T2 occurred in response to static loading in neutral alignment, with remarkable side- and depth-dependent variation in T2 changes; this decrease was more apparent in the medial femorotibial joints. In human knees with neutral alignment, the medial compartment is subjected to higher load than the lateral compartment because of the knee adduction moment in the stance phase[26,27]. Morrison *et al.* investigated the mechanics of knee joint during walking using a force-plate cinephotographic technique, and indicated that the greater part of the joint force was transmitted by the medial condyle[27]. Although there are species-specific variations in knee morphology and biomechanics, the biomechanical status may differ between the medial

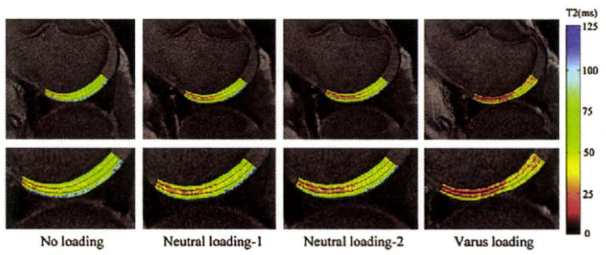


**Fig. 4.** Representative sagittal MRI of the medial femoral cartilage in the porcine knee at each condition. The femoral cartilage was subdivided into three zones using custom-made software. The lower figures showed the detail of femoral cartilage.

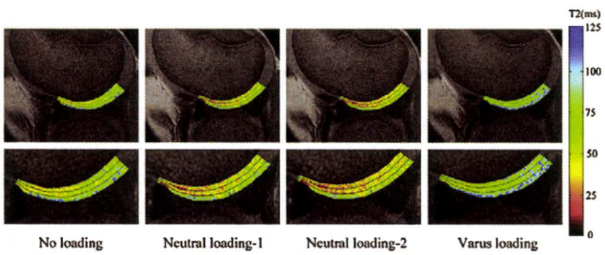


**Fig. 5.** Representative sagittal MRI of the lateral femoral cartilage in the porcine knee at each condition. The femoral cartilage was subdivided into three zones using custom-made software. The lower figures showed the detail of femoral cartilage.

**Table II**
T2 values in each zone under neutral loading-1 and neutral loading-2 ($N = 10$)

| Zones | Medial cartilage (ms) | | | Lateral cartilage (ms) | | |
|---|---|---|---|---|---|---|
| | Neutral loading-1 (SD) | Neutral loading-2 (SD) | Change (95% CI) | Neutral loading-1 (SD) | Neutral loading-2 (SD) | Change (95% CI) |
| Deep | 58.4 (5.2) | 57.4 (5.4) | −1.8 (−3.7, 0.0) | 60.2 (6.1) | 58.0 (6.9) | −3.7 (−7.4, 0.1) |
| Intermediate | 54.4 (7.4) | 53.9 (7.4) | −0.8 (−2.7, 1.1) | 59.6 (8.4) | 58.8 (9.0) | −1.4 (−3.8, 1.1) |
| Superficial | 63.1 (6.4) | 62.6 (7.2) | −1.1 (−2.8, 0.6) | 68.8 (9.0) | 67.1 (8.9) | −2.6 (−4.3, −0.9) |

At neutral loading-2, T2 maps and 3D SPGR images were obtained after compression was continued for 30 min following MR imaging at neutral loading-1, to examine the influence of loading duration on cartilage T2 measurements.
Changes were calculated as (values under neutral loading-2 − values under neutral loading-1)/values under neutral loading-1 × 100.
No significant difference between values under neutral loading-1 and neutral loading-2.

and lateral sides of the knee joint even at neutral alignment showing side-dependent T2 changes under loading.

Decrease in T2 was significantly larger in the intermediate cartilage zone than in the deep cartilage zone in both medial and lateral femorotibial joints. This depth-wise change in cartilage T2 under static loading may be related to different biomechanical functions of the cartilage zones. The deep zone of the cartilage comprises predominantly parallel collagen fibers aligned perpendicular to the subchondral plate (deep zone). The next zone of the cartilage comprises randomly oriented fibers (intermediate zone). The thin superficial zone of the cartilage comprises fibers aligned parallel to the articular surface (superficial zone)[22]. A radially oriented collagen network is responsible for the elastic properties of the cartilage, whereas the tangential arrangement of the collagen network essentially reflects shear forces within the loaded cartilage[28]. Using excised bone-cartilage plugs of juvenile pigs, Gründer *et al.* reported that under static loading MR intensity changed differently in three zones and the MR intensity of radial zone increased in which collagen fibers spread out and the portion of fibers oriented at magic angle with respect to the static magnetic field increased[8]. Rubenstein *et al.* observed an increase of cartilage T2 in the deep zone of excised cartilage plugs under static loading with the effect of increasingly obliquely oriented collagen fibers[9]. In contrast, Visser *et al.* assessed diffusion tensor imaging and cartilage T2 to observe adaptations of collagen fibers to mechanical compression in excised cartilage plugs and demonstrated compression led to the largest decreased T2 value in the superficial and transitional zone[29]. Our result that cartilage T2 values changed in layer-specific manner of three zones under static loading was similar to those previous studies, but predominant trend of increase or decrease of cartilage T2 by loading was different. Cartilage T2 in response to static loading was influenced by several factors, such as deformation of cartilage architecture, extrusion of water content, and relative increase of proteoglycan and collagen content within the cartilage[6,8,9,13,19]. Patterns and severity of those confounding factors under loading may be different between excised cartilage plugs and the whole-knee joint model in our study. Further investigation regarding layer-specific T2 value under loading will be required.

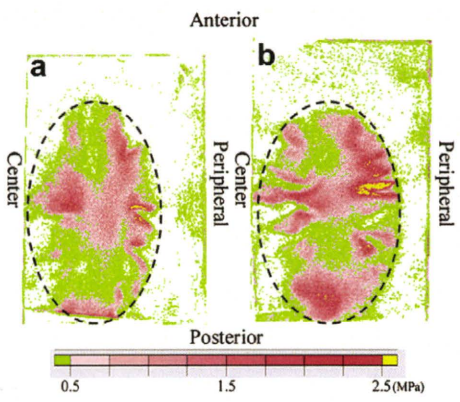


**Fig. 6.** Representative pressure distributions in pressure-sensitive films inserted under the medial femoral condyle. The color scale at the bottom shows values representing megapascals. (a) Under neutral loading-1 condition. (b) Under varus loading condition. Circle in dotted lines corresponds to a weight bearing area. Note that pressure concentration was shown more severely and diffusely along the medial meniscus under varus loading condition compared with neutral loading-1 condition.

These site-specific changes of cartilage T2 under static loading were remarkable when there was a change in varus alignment (varus loading). Guettler *et al.* investigated femorotibial pressure on eight fresh-frozen cadaveric knees and found that a relatively small degree of varus malalignment caused a dramatic alteration in articular surface contact pressure[30]. Our finding that cartilage T2 was further decreased in the medial joints but increased in the lateral joints under varus loading was in accordance with the biomechanical studies of Guettler *et al.*[30]. Significant correlation with joint pressure measurements and cartilage T2 values in the present study also indicated the usefulness of T2 change under static loading for biomechanical assessment. In patients with knee disorders, increased mechanical stress caused by malalignment is an important risk factor for progression of femorotibial osteoarthritis[26]. T2 mapping under loading may be a potent, non-invasive imaging tool for prognosis of osteoarthritis progression by evaluating altered loading condition imposed on the cartilage resulting from abnormal knee alignment such as varus deformity, and degenerative or traumatic disorders of the meniscus[18].

Cartilage deformation under loading occurs as a function of time and magnitude of load application. Herberhold *et al.* studied deformational behavior of the articular cartilage under static loading of 150% of the body weight with femoropatellar knee imaging *ex vivo*[10]. The deformations of the patellar and femoral cartilages after 8 min of compression were 25%–30% of the final deformation of these cartilages after 214 min of compression. We compared cartilage T2 under the same static loading conditions after 5 min (neutral loading-1) and 30 min (neutral loading-2) of compression to examine the influence of loading duration on cartilage T2 measurements. There was no significant difference in T2 values between neutral loading-1 and neutral loading-2 in any zone. This may indicate that equilibrium of cartilage deformation in response

**Table III**
Correlation coefficient between T2 values and contact pressure in each zone under neutral loading-1 and varus loading ($N = 10$)

| Zones | Neutral loading-1 | Slope | *P*-Value | Varus loading | Slope | *P*-Value |
|---|---|---|---|---|---|---|
| Medial cartilage | | | | | | |
| Deep | −0.17 | −0.11 | 0.647 | −0.12 | −0.13 | 0.741 |
| Intermediate | −0.64 | −0.66 | 0.031* | −0.49 | −0.42 | 0.047* |
| Superficial | −0.48 | −0.47 | 0.048* | −0.55 | −0.53 | 0.043* |
| Lateral cartilage | | | | | | |
| Deep | −0.23 | −0.27 | 0.533 | −0.39 | −0.41 | 0.179 |
| Intermediate | −0.48 | −0.59 | 0.049* | −0.78 | −0.67 | 0.005* |
| Superficial | −0.41 | −0.44 | 0.184 | −0.73 | −0.80 | 0.015* |

* Significant correlation between T2 values and contact pressure.

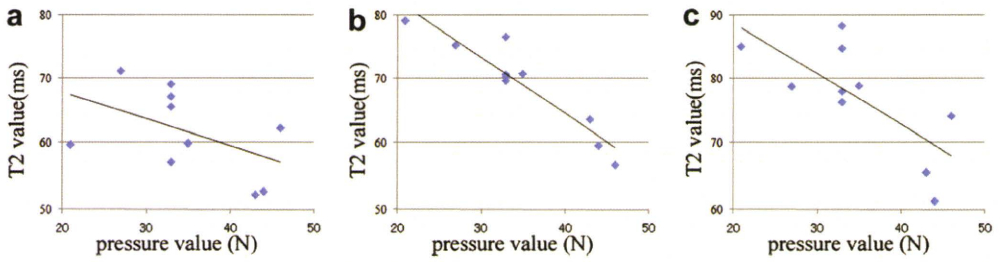


**Fig. 7.** The correlation between T2 values and contact pressure in the lateral cartilage on varus loading. (a) deep zone (b) intermediate zone (c) superficial zone.

to loading was mostly achieved in a short duration in the present study. A relatively low magnitude of applied load (approximately one-third of the body weight) may shorten the duration to reach the final equilibrium condition of cartilage deformation.

Our study had several limitations. First, the cartilage boundary for ROI placements was manually defined for calculation of cartilage T2. However, cartilage boundary was easily determined presumably because of the relatively high in-plane resolution, high signal contrast between the cartilage and adjacent subchondral bone, and use of anterior and posterior menisci as anatomical landmarks. The intra-observer and inter-observer reproducibility of cartilage T2 measurements in the present study ranged from 3% to 5% at each zone, which was comparable to results obtained in previous studies[13,31]. We detected significant decreases in cartilage T2 values at intermediate zone under neutral loading-1 and varus loading, which were more than the double of the reproducibility of T2 measurements. Given the acceptable reproducibility of the present measurements to detect significant change of cartilage T2 by loading, we consider that ROIs were reliably defined in the present study. Second, the composition and thickness of the articular cartilage in different species may vary with different load-bearing patterns, and the *ex vivo* whole-knee model did not take into account surrounding muscle action (e.g., contraction of quadriceps or hamstrings) or forces from surrounding ligamentous restraints. Severity and localization of change in the MRI measurements in association with loading or varus alignment may be different in human knee imaging *in vivo*. In the present study, distribution patterns of T2 mapping with lower T2 in the deep zone and higher T2 in the superficial zone without loading were similar to those of human adult cartilage *in vivo*[32,33]. We believe that this model had a water distribution pattern similar to human cartilage and allowed investigation of the load response of cartilage extracellular matrix mainly with respect to water distribution by T2 mapping. Third, although time-dependent compressive creep and stress relaxation behavior of cartilage occur in the biphasic theory[34], we validated accuracy of the device using an incompressible rod because a testing material which had biomaterial property similar to viscoelastic property of cartilage was not available. In the present study, the analysis of the cartilage deformation of the weight-bearing area in the SPGR image corresponding T2 map showed mean reduction of approximately 0.2 mm thickness under neutral loading-1, and approximately 0.4 mm thickness under varus loading compared with the initial thickness. Compression of viscoelastic foam material by 10 mm resulted in providing continuous compression force to the incompressible rod by 134 N–140 N. Loss of compression of the foam material by 0.4 mm due to cartilage deformation was assumed to decrease the compression force about 4.8 N from additional experiments (data was not shown). As the cartilage deformation of viscoelastic phenomena was relatively small compared with the displacement of the foam material, we considered the result of the preliminary test with incompressible rod provided similar results regarding the accuracy of the device. Fourth, cartilage T2 was evaluated under viscoelastic phenomena such as stress relaxation, but the pressure-sensitive film left inside a joint recorded the peak pressures during the loading period. Although real-time measurement of pressure was impossible for the pressure-sensitive film, this film has advantages in matching the sheet form to convex of the knee joint and minimizing change of biomechanical condition by placing the thin film into the knee joint. With this limitation in mind, we investigated how femoral cartilage T2 changed in layer-specific manner using the realistic whole-knee joint model when cartilage surface was compressed by static loading and varus knee alignment condition. Care should be taken for interpretation of the present finding that direct correlation between depth-wise distribution of strain and T2 value within the cartilage was not clarified in this study. Finally, we also have interest on analysis of T2 changes of the tibial cartilage in association with the opposing femoral cartilage when the load is applied. However, comparison of the T2 mapping in the same location of the tibial cartilage between the neutral loading and varus loading might be difficult because it was difficult to place the same saggital imaging plane in the oblique-positioned tibia at varus loading, to the imaging plane in the neutral-positioned tibia. In contrast, the position of the femur was constant throughout the experiment (no loading, neutral loading and varus loading). In our layer-specific analysis of cartilage T2, ROI placement in the same anatomical location was important to reveal accurate change of T2 value in association with loading conditions. Furthermore, thickness of the tibial cartilage, ranging 1 mm–2 mm, was small as compared with the femoral cartilage thickness ranging 3 mm–4 mm. In the present study, in-plane resolution of T2 maps was 0.26 mm × 0.39 mm. Due to thin thickness, we consider that adequate evaluation of T2 values in the three subdivided layers along the cartilage depth was difficult in the tibial cartilage. From these concerns, we focused on analysis of T2 changes of the femoral cartilage in the present study.

In conclusion, our results indicated that quantitative assessment of MRI for the cartilage differed in various physiological conditions, and T2 mapping under static loading allowed non-invasive biomechanical assessment of site-specific stress distribution in the cartilage. Although further investigations will be required, evaluation of dynamic changes in the collagen architecture, along with evaluation of water influx or efflux through the cartilage in response to physiological loading, may provide more sensitive and detailed assessment of degenerative pathological changes and load-bearing function of the cartilage compared to mere static assessment of solid matrix and water content.

## Conflict of interest

The authors have no conflict of interest.

## Acknowledgments

The authors wish to thank Yasuo Hara, Department of Technology Development, IVTeC, Japan, for technical assistance, and Ichiro Nakahara, Department of Orthopaedic Surgery, Osaka

University Medical School, Osaka, Japan, for his assistance in image analysis.

This work was supported in part by a program "Collaborative Development of Innovative Seeds" (6090026) from the Japan Science and Technology Agency and Grant-in-Aid for Scientific Research (19591757) of the Ministry of Education, Science and Culture in Japan.

## References

1. Mosher TJ, Dardzinski BJ, Smith MB. Human articular cartilage: influence of aging and early symptomatic degeneration on the spatial variation of T2-preliminary findings at 3 T. Radiology 2000;214:259–66.
2. Dunn TC, Lu Y, Jin H, Ries MD, Majumdar S. T2 relaxation time of cartilage at MR imaging: comparison with severity of knee osteoarthritis. Radiology 2004;232:592–8.
3. Burstein D, Bashir A, Gray ML. MRI techniques in early stages of cartilage disease. Invest Radiol 2000;35:622–38.
4. Li X, Benjamin M, Link TM, Castillo DD, Blumenkrantz G, Lozano J, *et al. In vivo* $T_{1\rho}$ and $T_2$ mapping of articular cartilage in osteoarthritis of the knee using 3 T MRI. Osteoarthritis Cartilage 2007;15:789–97.
5. Li X, Pai A, Blumenkrantz G, Carballido-Gamio J, Link T, Benjamin C, *et al.* Spatial distribution and relationship of $T_{1\rho}$ and $T_2$ relaxation times in knee cartilage with osteoarthritis. Magn Reson Med 2009;61:1310–8.
6. Mosher TJ, Smith HE, Collins C, Liu Y, Hancy J, Dardzinski BJ, *et al.* Change in knee cartilage T2 at MR imaging after running: a feasibility study. Radiology 2005;234:245–9.
7. Eckstein F, Tieschky M, Faber SC, Haubner M, Kolem H, Englmeier KH, *et al.* Effect of physical exercise on cartilage volume and thickness *in vivo*: MR imaging study. Radiology 1998;207:243–8.
8. Gründer W, Kanowski M, Wagner M, Werner A. Visualization of pressure distribution within loaded joint cartilage by application of angle-sensitive NMR microscopy. Magn Reson Med 2000;43:884–91.
9. Rubenstein JD, Kim JK, Henkelman RM. Effects of compression and recovery on bovine articular cartilage: appearance on MR images. Radiology 1996;201:843–50.
10. Herberhold C, Faber S, Stammberger T, Steinlechner M, Putz R, Englmeier KH, *et al.* In situ measurement of articular cartilage deformation in intact femoropatellar joints under static loading. J Biomech 1999;32:1287–95.
11. Kaufman JH, Regatte RR, Bolinger L, Kneeland JB, Reddy R, Leigh JS. A novel approach to observing articular cartilage deformation *in vitro via* magnetic resonance imaging. J Magn Reson Imaging 1999;9:653–62.
12. Menezes NM, Gray ML, Hartke JR, Burstein D. $T_2$ and $T_{1\rho}$ MRI in articular cartilage systems. Magn Reson Med 2004;51: 503–9.
13. Liess C, Lüsse S, Karger N, Heller M, Glüer CC. Detection of changes in cartilage water content using MRI T2-mapping *in vivo*. Osteoarthritis Cartilage 2002;10:907–13.
14. Hayashi K, Takano H, Matsuda T, Umezu M. Mechanical stability of elastomeric polymers for blood pump applications. J Biomed Mater Res 1985;19:179–93.
15. Fukubayashi T, Kurosawa H. The contact area and pressure distribution of the knee. Acta Orthop Scand 1980;51:871–9.
16. Wu JZ, Herzog W, Epstein M. Effects of inserting a pressensor film into articular joints on the actual contact mechanics. J Biomech Eng 1998;120:655–9.
17. Wayne JS, Kraft KA, Shields KJ, Yin C, Owen JR, Disler DG. MR imaging of normal and matrix-depleted cartilage: correlation with biomechanical function and biochemical composition. Radiology 2003;228:493–9.
18. Nishii T, Kuroda K, Matsuoka Y, Sahara T, Yoshikawa H. Change in knee cartilage T2 in response to mechanical loading. J Magn Reson Imaging 2008;28:175–80.
19. Nag D, Liney GP, Gillespie P, Scerman KP. Quantification of T2 relaxation changes in articular cartilage with in situ mechanical loading of the knee. J Magn Reson Imaging 2004;19:317–22.
20. Donnan FG. The theory of membrane equilibria. Chem Rev 1924;1:73–90.
21. Maroudas A, Schneiderman R. "Free" and "exchangeable" or "trapped" and "non-exchangeable" water in cartilage. J Orthop Res 1987;5:133–8.
22. Rubenstein JD, Kim JK, Morova-Protzner I, Stanchev PL, Henkelman RM. Effects of collagen orientation on MR imaging characteristics of bovine articular cartilage. Radiology 1993;188:219–26.
23. Peto S, Gillis P. Fiber-to-field angle dependence of proton nuclear magnetic relaxation in collagen. Magn Reson Imaging 1990;8:705–12.
24. Reiter DA, Lin PC, Fishbein KW, Spencer RG. Multicomponent T2 relaxation analysis in cartilage. Magn Reson Med 2009;61:803–9.
25. Hardy PA, Ridler AC, Chiarot CB, Plewes DB, Henkelman RM. Imaging articular cartilage under compression – cartilage elastography. Magn Reson Med 2005;53:1065–73.
26. Eckstein F, Wirth W, Hudelmaier M, Stein V, Lengfelder V, Cahue S, *et al.* Patterns of femorotibial cartilage loss in knees with neutral, varus, and valgus alignment. Arthritis Rheum 2008;59:1563–70.
27. Morrison JB. The mechanics of the knee joint in relation to normal walking. J Biomech 1970;3:51–61.
28. Harrington IJ. Static and dynamic loading patterns in knee joints with deformities. J Bone Joint Surg Am 1983;65: 247–59.
29. Visser SK, Crawford RW, Pope JM. Structual adaptations in compressed articular cartilage measured by diffusion tensor imaging. Osteoarthritis Cartilage 2008;16:83–9.
30. Guettler J, Glisson R, Stubbs A, Jurist K, Hoggins L. The triad of varus malalignment, meniscectomy, and chondral damage: a biomechanical explanation for joint degeneration. Orthopedics 2007;30:558–66.
31. Glaser C, Mendlik T, Dinges J, Weber J, Stahl R, Trumm C, *et al.* Global and regional reproducibility of T2 relaxation time measurements in human patellar cartilage. Magn Reson Med 2006;56:527–34.
32. Nishii T, Tanaka H, Sugano N, Sakai T, Hananouchi T, Yoshikawa H. Evaluation of cartilage matrix disorders by T2 relaxation time in patients with hip dysplasia. Osteoarthritis Cartilage 2008;16:227–33.
33. Smith HE, Mosher TJ, Dardzinski BJ, Collins BG, Collins CM, Yang QX, *et al.* Spatial variation in cartilage T2 of the knee. J Magn Reson Imaging 2001;14:50–5.
34. Mow VC, Kuei SC, Lai WM, Armstrong CG. Biphasic creep and stress relaxation of articular cartilage in compression? Theory and experiments. J Biomech Eng 1980;102:73–84.

# Influence of Knee Positions on $T_2$, $T^*_2$, and dGEMRIC Mapping in Porcine Knee Cartilage

Toshiyuki Shiomi,[1] Takashi Nishii,[1,2]* Akira Myoui,[1,3] Hideki Yoshikawa,[1] and Nobuhiko Sugano[1,2]

**We examined the influence of flexed knee positions on cartilage MR assessments. Sagittal $T_2$, $T^*_2$, and delayed gadolinium-enhanced MRI of cartilage (dGEMRIC) maps of the femoral cartilage were obtained in eight 6-month-old porcine femorotibial joints in the extended knee position (position A: flexion 0° and femoral shaft in parallel with the amplitude of static field), flexed knee position (position B: flexion 40° and femoral shaft oriented at 40° to the amplitude of static field), and oblique-placed knee-extended position (position C: flexion 0° and femoral shaft oriented at 40° to the amplitude of static field). Comparison of the MR parameters between positions A and C showed isolated influence of the magic-angle effect, and comparison between positions A and B showed effects of knee flexion. Proteoglycan and hydroxyproline content in cartilage specimen at each region of interest had no significant correlation with $T_2$, $T^*_2$, and dGEMRIC values. At the central zone, located on a weight-bearing area and parallel to the amplitude of static field, $T_2$/$T^*_2$/dGEMRIC values increased by 6.8/11/0.8% at position C and by 24/44/31% at position B compared with position A. There was a significant increase in $T_2$ and $T^*_2$ values at position B compared with those at position A. The substantial changes in $T_2$, $T^*_2$, and dGEMRIC were shown in response to knee flexion, presumably due to the compounding influence of the magic-angle effect and change in the intra-articular biomechanical condition. Magn Reson Med 64:707–714, 2010. © 2010 Wiley-Liss, Inc.**

**Key words: MRI; knee cartilage; $T_2$; $T^*_2$; dGEMRIC**

Knee imaging using quantitative MRI techniques, such as $T_2$ (1,2), $T^*_2$ (3), delayed gadolinium-enhanced MRI of cartilage (dGEMRIC) (4,5), and $T_1$ in the rotating frame (T1rho) (6), achieved great advancements in noninvasive assessments of the articular cartilage, particularly about matrix compositions and degenerative changes. Sensitive evaluations in water, collagen, or proteoglycan content and collagenous arrangements in the cartilage in vivo were obtained using the aforementioned techniques, without performing destructive retrieval analysis.

In most clinical studies, quantitative MR assessments were performed in the extended knee position, with the longitudinal axis of the femur and tibia aligned in parallel with the amplitude of static magnetic field ($B_0$). Recently, knee kinematic investigations using MRI at flexion in various angles have provided valuable information regarding the physiological and pathological conditions of intra-articular structures and their varied interactions among the articular cartilage, meniscus, and ligaments (7,8). Flexion of the knee joints resulted in a significantly different tibiofemoral contact area between healthy and injured knee joints, depending on the flexion angle. In such cases, by reflecting on the concomitant change of water content or deformation of collagenous arrangements in the cartilage (9–11), quantitative MR techniques may be effective for evaluating the biomechanical environment of articular cartilage in association with knee movements.

Quantitative MR evaluation in knee kinematic investigations, however, may encounter difficulties due to the magic-angle effect. Angular changes in the femoral and tibial positioning with respect to $B_0$ may cause a substantial localized change in the MR signal intensity due to the magic-angle effect. In prior experimental studies using excised cartilage specimens, a strong orientation dependence on the relaxation time of articular cartilage in MRI, especially for $T_2$, was observed (12). Maximum effect of $T_2$ elongation was obtained when the collagen fibers in the cartilage were oriented at ~55° relative to $B_0$. Clinically, focally increased signals observed on short echo time images of cartilage with curved articular surfaces such as the femoral condyle were partly accounted for by the magic-angle effect. Therefore, it may be difficult to distinguish between the changes in quantitative MR assessments of the femoral cartilage associated with knee flexion due to alteration of content or structure in water or extracellular matrix within the cartilage and those caused by the magic-angle effect.

Previous experimental investigations using isolated, excised cartilage specimens explored the effect of magic angle on MR relaxation time in detail. To our knowledge, however, no studies have documented an orientation dependence of cartilage relaxation time associated with the flexion of the knee in clinical situations, with a whole joint model retaining the meniscus, ligaments, and the capsule in situ. The purpose of this study is to examine the influence of flexed knee positions on cartilage assessments by $T_2$, $T^*_2$, and dGEMRIC mapping, using cadaver porcine femorotibial joints, and to correlate articular

[1]Department of Orthopaedic Surgery, Osaka University Medical School, Osaka, Japan.

[2]Department of Orthopaedic Medical Engineering, Osaka University Medical School, Osaka, Japan.

[3]Medical Center for Translational Research, Osaka University Hospital, Osaka, Japan.

Grant sponsor: Japan Science and Technology Agency; Grant number: 6090026 (Collaborative Development of Innovative Seeds program); Grant sponsor: Ministry of Education, Science and Culture in Japan; Grant number: 19591757.

*Correspondence to: Takashi Nishii, M.D., Department of Orthopaedic Medical Engineering, Osaka University Medical School, 2-2 Yamadaoka, Suita, Osaka 565-0871, Japan. E-mail: nishii@ort.med.osaka-u.ac.jp

Received 11 March 2009; revised 5 February 2010; accepted 7 March 2010.

DOI 10.1002/mrm.22469

Published online 9 June 2010 in Wiley Online Library (wileyonlinelibrary.com).

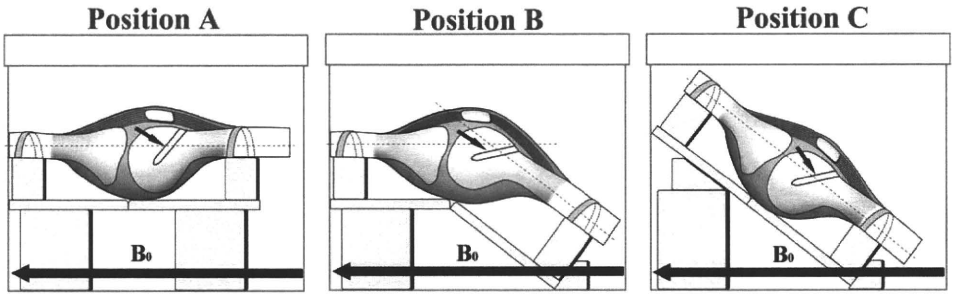


FIG. 1. Femorotibial porcine knee joints in the extended knee position (position A: flexion 0° and the femoral shaft in parallel with $B_0$), flexed knee position (position B: flexion 40° and the femoral shaft oriented at 40° to $B_0$), and oblique-placed knee-extended position (position C: flexion 0° and the femoral shaft oriented at 40° to $B_0$). A small cylindrical bone defect (arrow) was made in the middle of the lateral and medial femoral condyle as a fiducial mark.

biochemical compositions, such as proteoglycan and collagen content, in MRI parameters.

## MATERIALS AND METHODS

### Preparation of Porcine Specimens

Eight fresh knee joints were harvested en bloc with intact capsule and surrounding muscle from 6-month-old pigs and stored at −40°C. On the day of MRI, the specimens were thawed at room temperature and a small cylindrical bone defect was made in the middle of the lateral and medial femoral condyle as a fiducial mark. First, the muscle was stripped from the anterior side of the femoral shaft up to the upper end of the femoral condyle and the bone defect was made using a 3 mm-diameter from the upper anterior end to the center portion of the femoral condyle. The defect did not reach the femoral articular cartilage and the subchondral bone to eliminate an artificial effect on MRI by the scar. Then, a wooden stick of the corresponding size was introduced into the bone defect. This bone defect was used to obtain reproducible identification of the same imaging plane and for defining the regions of interest (ROIs) in subsequent imaging sequences. During the procedure, care was taken to preserve the capsule and the medial and lateral collateral ligament around the knee joint. The specimen was fixed in an acryl box filled with phosphate-buffered saline, and the air in the box was removed. The knee joint, sealed by the capsule, was also filled with phosphate-buffered saline by injection via the capsule.

### MRI

MRI was performed using a 1.5-T MRI system (MAGNETOM Espree; Siemens, Erlangen, Germany) and a standard 14-cm-diameter quadrature knee coil (Siemens). The MR system was equipped with $4 \times 10^{-4}$ T/cm gradients. The porcine knee was placed in a supine, head-first orientation in the center of the coil. Sagittal $T_2$ and $T_2^*$ maps were first obtained for the lateral and medial femorotibial joints in the extended knee position (position A: flexion 0° and the femoral shaft in parallel with $B_0$) and then in the flexed knee position (position B: flexion ~40° and the femoral shaft, oriented at 40° to $B_0$) (Fig. 1). In both knee positions, the tibia was placed in parallel with $B_0$. A flexion angle of 40° was confirmed, using a measurement device. During analyses of the MR images, the actual flexion angle at position B averaged 41.5° ± 2.5°. Then, the knee joints were immersed and equilibrated in 1-mM gadolinium-diethylene triamide pentaacetic acid solution (Magnevist; Schering AG, Germany) for 3 h. We determined the immersion time based on previous studies (13,14) in which nearly maximal increase of $T_1$-weighted signal intensity was obtained by 2.5-h immersion of cartilage specimen in gadolinium-diethylene triamide pentaacetic acid solution. Then, sagittal dGEMRIC maps were obtained in the same imaging plane and knee positions (positions A and B). In all mappings, the corresponding sagittal plane was determined to include the fiducial mark.

In six of the eight knees, the sagittal $T_2$, $T_2^*$, and dGEMRIC maps in the extended knee position (flexion 0°) and the femoral shaft oriented at 40° to $B_0$ (position C) were also obtained to evaluate the isolated influence of the magic-angle effect (Fig. 1).

$T_2$ and $T_2^*$ maps were calculated using a monoexponential fit from two-dimensional multiecho spin-echo sequences (pulse repetition time, 4000 msec; 10 echoes between 18.7 and 187 msec; field of view, 10 cm; matrix, 256 × 256; slice thickness, 3 mm; signal averaging, 2; acquiring time, 13 min 9 sec) and two-dimensional multiecho gradient echo sequences (pulse repetition time, 1500 ms; nine echoes between 10 and 72.96 msec; field of view, 10 cm; matrix, 256 × 256; slice thickness, 3 mm; signal averaging, 2; acquiring time, 6 min 24 sec), respectively. Frequency-selective fat-suppression technique was used to minimize the chemical shift artifact at the cartilage–bone interface. Frequency encoding was oriented in the cranial-to-caudal direction. In a preliminary experiment using 10 excised distal femurs of juvenile pigs, we compared $T_2$ measurements on several ROIs of the femoral cartilage with and without fat-suppression technique. The frequency-selective fat-suppression technique had no significant influence on $T_2$ measurements on the femoral cartilage. dGEMRIC maps were calculated from an inversion-recovery fast spin-echo sequence (pulse repetition time, 1800 ms; echo time, 14 ms; inversion time = 50–1680 msec; echo train length, 5; field of

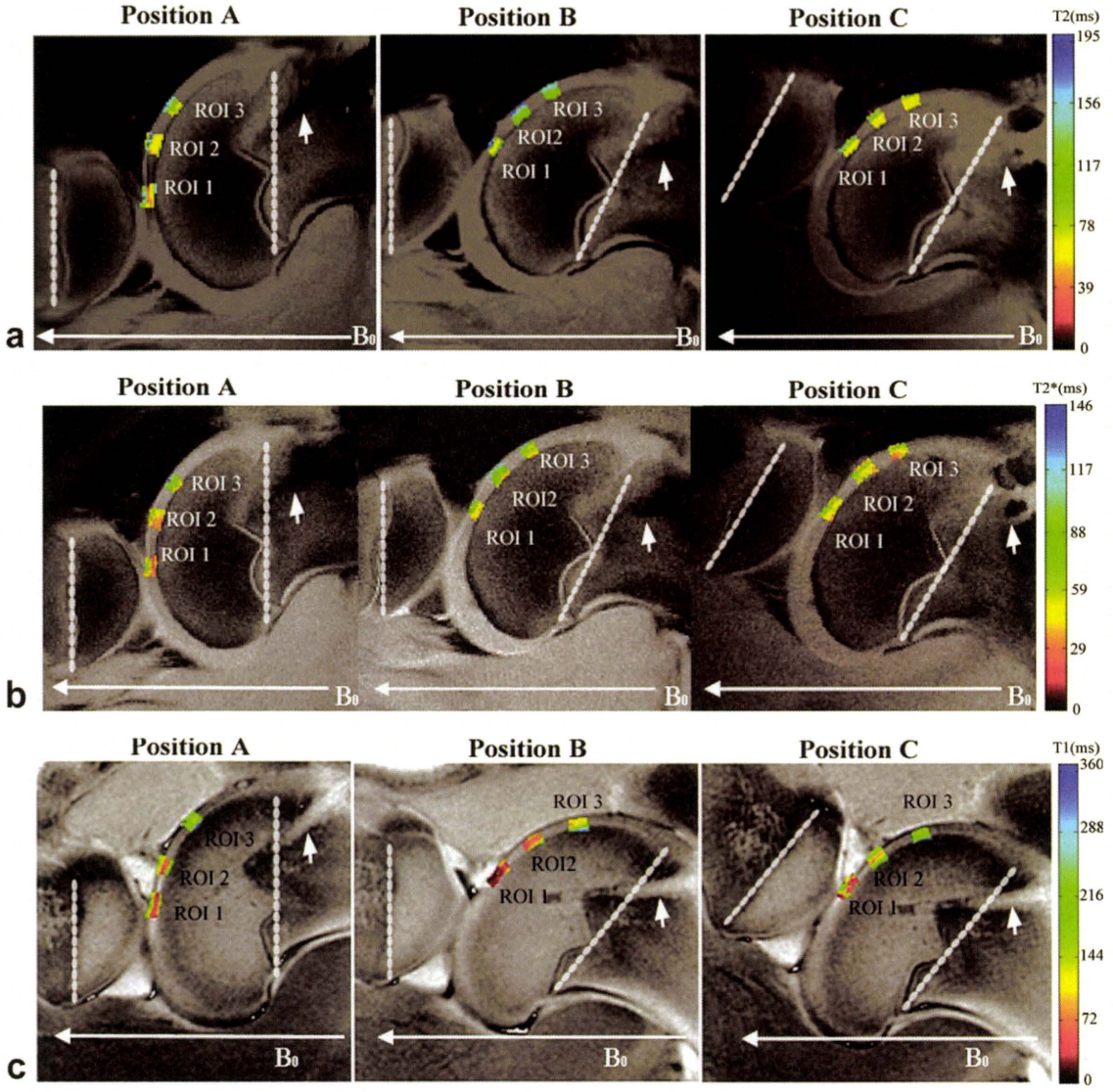


FIG. 2. Sagittal $T_2$ (a), $T_2^*$(b), and dGEMRIC (c) maps, respectively, with definition of ROIs 1, 2, and 3 at positions A, B, and C. White arrowheads indicate fiducial marks. Dotted lines are perpendicular to the femoral and tibial shaft.

view, 10 cm; matrix, 256 × 256; slice thickness, 3 mm; signal averaging, 2; acquiring time, 11 min 5 sec). In all sequences, one sagittal image passing through the middle of the medial femoral condyle and one sagittal image passing through the middle of the lateral femoral condyle with the fiducial marks were obtained. All data analyses were conducted using in-house MatLab scripts (MathWorks Inc., Natick, MA).

### Image Analysis

In each mapping at knee position A, three ROIs were manually defined on the medial and lateral femoral cartilages (Fig. 2): ROI 1 was covered by the anterior meniscus in the weight-bearing area and was parallel to $B_0$, and ROIs 2 and 3 were free from the weight-bearing area and oriented at 25° and 50° to $B_0$, respectively. Placement of the three ROIs in the mappings at knee positions B and C were matched with the ROIs at knee position A, using the fiducial mark. Definitions of ROIs were repeated twice by a single observer (T.S.), and the $T_2$, $T_2^*$, and dGEMRIC values of each medial and lateral ROI were averaged. The values of ROI 2 from the lateral femoral condyle were excluded from the analysis because the region was anatomically covered with fibrous tissue. Reproducibility between the two measurements was calculated as the coefficient of variation (standard deviation/mean × 100%), and mean reproducibility was calculated as the root mean square average for all specimens. Reproducibility at each ROI ranged from 3.5 to 5.0% in $T_2$, 3.9 to 5.6% in $T_2^*$, and 3.5 to 5.0% in dGEMRIC measurements. To investigate influence of equilibration time for dGEMRIC assessment in en bloc knee joints, dGEMRIC values were measured repeatedly after immersion in 1-mM gadolinium-diethylene triamide pentaacetic acid solution both for 3 h and 24 h in another two porcine knee joints.

$T_2$, $T_2^*$, and dGEMRIC values for extended (position A) and flexed (position B) knee positions at each ROI were compared using the Wilcoxon test to estimate the

Table 1
$T_2$, $T_2^*$, and dGEMRIC Values in Each ROI (Mean ± SD) at Knee Positions A and B ($N = 8$)*

| Zones | | Position A | Position B | Change (%) | P value |
|---|---|---|---|---|---|
| $T_2$ value (msec) | ROI 1 | 80.7 ± 8.8 | 97.9 ± 16.5 | 24.1 ± 27.9 | 0.014[a] |
| | ROI 2 | 98.6 ± 11.6 | 98.5 ± 12.2 | 0.1 ± 6.7 | 0.128 |
| | ROI 3 | 112.7 ± 25.4 | 88.9 ± 17.5 | −17.9 ± 19.2 | 0.004[a] |
| $T_2^*$ value (msec) | ROI 1 | 33.0 ± 9.7 | 44.3 ± 8.2 | 44.4 ± 47.3 | 0.002[a] |
| | ROI 2 | 46.0 ± 9.5 | 58.5 ± 7.2 | 29.9 ± 20.4 | 0.012[a] |
| | ROI 3 | 52.6 ± 17.8 | 49.6 ± 14.7 | −2.9 ± 23.4 | 0.379 |
| dGEMRIC value (msec) | ROI 1 | 166.3 ± 80.5 | 188.0 ± 65.4 | 30.6 ± 69.2 | 0.277 |
| | ROI 2 | 244.3 ± 86.3 | 239.1 ± 58.1 | 2.8 ± 18.9 | 0.674 |
| | ROI 3 | 277.1 ± 64.3 | 244.6 ± 62.3 | −10.5 ± 18.4 | 0.234 |

*Changes were calculated as (values at position B − values at position A)/values at position A × 100.
[a]Significant difference between values at positions A and B.

influence of posture change that occurs naturally during clinical examinations. MR quantitative values with knee extension at positions A and C at each ROI were compared using the Wilcoxon test to estimate the isolated influence of the magic-angle effect that occurs due to a relative change in the femoral articular cartilage against $B_0$. Relationships among changes in the $T_2$, $T_2^*$, and dGEMRIC values associated with knee flexion were evaluated using the Spearman correlation coefficient. A probability value of $P < 0.05$ was considered statistically significant.

### Biochemical Analysis

After MRI, a biochemical assay of the cartilage specimen at each ROI was performed to determine the proteoglycan and collagen content. Using a cylindrical punch, full-thickness cartilage disks (diameter of 4 mm) without subchondral bone were removed from the knees, matching each ROI. The cartilage was analyzed to determine the concentrations of hydroxyproline, a measure of collagen content, and sulfated glycosaminoglycan, a measure of proteoglycan content. For assessment of hydroxyproline content, the cartilage was hydrolyzed with 6-N hydrochloric acid at 130°C for 6 h, neutralized, and analyzed using a colorimetric procedure at a wavelength of 557 nm. For analysis of sulfated glycosaminoglycan content, the cartilage was digested in papain solution and then assessed using the dimethylmethylene blue binding assay at a wavelength of 535 nm.

### Polarized Light Microscopy

Histological assessment of birefringence in 6-month-old porcine femoral cartilage specimens was conducted using polarized light microscopy. Birefringence of articular cartilage is suggested to be an index of the combined effect of collagen content and network organization (15). Polarized light microscopy measurement was conducted using a VHX-1000 digital microscope (Keyence, Japan) equipped with a VH-Z100UW universal zoom lens (Keyence). To determine collagen anisotropy, a cartilage sample, which was formalin fixed and treated with enzymatic removal of proteoglycans and cut into 5-μm-thick microscopic sections, was imaged at various orientations of crossed polarizers, and the maximum contrast of birefringence was recorded.

## RESULTS

In the investigation for influence of equilibration time for dGEMRIC assessment, the average dGEMRIC values of ROIs 1/2/3 for the lateral and medial femorotibial joints were 174/193/206 msec at 3-h immersion and 171/182/201 msec at 24-h immersion. Immersion in contrast agent for 3 h was assumed to be sufficient to equilibrate the articular cartilage of en bloc knee joints in dGEMRIC assessment.

Table 1 shows $T_2$, $T_2^*$, and dGEMRIC values in each ROI between knee position A and position B, and Table 2 shows those values between knee position A and position C. At position A, the average quantitative values of ROIs 1/2/3 were 81/99/113 msec for $T_2$, 33/46/53 msec

Table 2
$T_2$, $T_2^*$, and dGEMRIC Values in Each ROI (Mean ± SD) at Knee Positions A and C ($N = 6$)*

| Zones | | Position A | Position B | Change (%) | P value |
|---|---|---|---|---|---|
| $T_2$ value (msec) | ROI 1 | 81.3 ± 15.0 | 84.7 ± 10.1 | 6.8 ± 19.7 | 0.374 |
| | ROI 2 | 95.2 ± 8.5 | 99.7 ± 10.4 | 5.2 ± 11.9 | 0.074 |
| | ROI 3 | 105.2 ± 22.3 | 90.5 ± 12.4 | −12.1 ± 13.2 | 0.012[a] |
| $T_2^*$ value (msec) | ROI 1 | 30.6 ± 9.6 | 33.5 ± 11.8 | 11.2 ± 23.3 | 0.224 |
| | ROI 2 | 43.5 ± 6.5 | 50.2 ± 11.0 | 15.1 ± 16.5 | 0.075 |
| | ROI 3 | 47.8 ± 15.6 | 43.8 ± 13.9 | −6.7 ± 13.7 | 0.077 |
| dGEMRIC value (msec) | ROI 1 | 179.8 ± 84.1 | 179.4 ± 84.0 | 0.8 ± 13.9 | 0.875 |
| | ROI 2 | 233.7 ± 98.3 | 228.5 ± 89.7 | −1.4 ± 8.3 | 0.753 |
| | ROI 3 | 264.7 ± 58.5 | 229.3 ± 61.7 | −11.4 ± 20.4 | 0.084 |

*Changes were calculated as (values at position C − values at position A)/values at position A × 100.
[a]Significant difference between values at positions A and C.